

## Electronic Supplementary Information<sup>†</sup>

# Supramolecular RNAi with Multifunctional siRNA Nanostructures

Michael Shaikhet,<sup>c</sup> Joshua O'Grady,<sup>a</sup> Filiz K. Collak,<sup>a,b</sup> Matthew Reynolds,<sup>c</sup> Anatoli Ianoul,<sup>a</sup>  
William G. Willmore,<sup>a,b,c</sup> Bruce C. McKay<sup>b,c</sup> and David Sabatino<sup>a,c,\*</sup>

<sup>a</sup>Department of Chemistry, <sup>b</sup>Department of Biology, and <sup>c</sup>Institute of Biochemistry,  
Carleton University, 1125 Colonel By Drive, Ottawa ON, K1S 5B6, Canada

\*Corresponding author

e-mail: [david.sabatino@carleton.ca](mailto:david.sabatino@carleton.ca)

### Table of Contents

<b>1. Materials and Methods</b> .....	S3
1.1. Materials.....	S3
1.2. Solid phase synthesis of RNA templates.....	S3
1.3. Fluorochrome labelling of RNA.....	S5
1.4. UV-Vis spectroscopy.....	S6
1.5. Reversed-phase ion-pairing high performance liquid chromatography.....	S6
1.6. Mass spectrometry.....	S6
1.7. RNA hybridization.....	S7
1.8. Denaturing polyacrylamide gel electrophoresis (PAGE).....	S7
1.9. Native PAGE.....	S8
1.10. Circular dichroism spectroscopy.....	S8
1.11 Thermal denaturation.....	S9
1.12 Fluorescence spectroscopy.....	S9
1.13 Transmission electron microscopy and energy dispersive X-ray spectroscopy.....	S9
1.14 Dynamic light scattering and zeta potential measurements.....	S10

1.15 Atomic Force Microscopy.....	S10
1.16 Raman Microspectroscopy.....	S11
1.17 Cell culture.....	S12
1.18 siRNA transfections.....	S12
1.19 Flow cytometry.....	S12
1.20 Confocal microscopy.....	S13
1.21 Fluorescence microscopy.....	S14
1.22 RNA isolation and quantitative reverse transcription polymerase chain reaction.....	S15
1.23 Protein isolation and western blots.....	S16
1.24 Cell viability.....	S16
1.25 Statistical analysis.....	S17
<b>2. Supplementary data</b>	
<b>Table S1.</b> GRP silencing RNA sequences.....	S18
<b>Table S2.</b> Characterization data.....	S18
<b>Table S3.</b> List of forward and reverse primer sequences for qRT PCR.....	S19
<b>Table S4.</b> NCBI BLAST (blastn) against the human RefSeq RNA database.....	S19
<b>Table S5.</b> Size and height measurements by AFM.....	S20
<b>Figures S1-S15.</b> Liquid chromatography mass spectrometry data.....	S21
<b>Figures S16-S18.</b> Native PAGE analysis.....	S36
<b>Figure S19-S23.</b> UV-Vis spectroscopy analysis.....	S38
<b>Figures S24-S25.</b> Fluorescence spectroscopy analysis.....	S41
<b>Figure S26.</b> Raman spectroscopy analysis.....	S42
<b>Figure S27.</b> Supplemental TEM images.....	S43
<b>Figure S28.</b> AFM analysis.....	S44
<b>Figure S29.</b> Fluorescence microscopy analysis.....	S45
<b>Figures S30-S40.</b> Western blot images.....	S46
<b>Figure S41.</b> Brightfield images from the Incucyte™.....	S57

## 1.1 Materials

Solid phase RNA synthesis reagents were obtained from ChemGenes Corporation (Wilmington, MA, USA) and were all sufficiently pure for direct use. Additional solvents, chemical synthesis reagents, and other chemistry materials were obtained from Avantor VWR, Millipore Sigma Aldrich and Thermo Fisher Scientific.

## 1.2 Solid-phase synthesis of RNA templates

The RNA sequences were synthesized on a K&A H-8 DNA/RNA Automated Synthesizer (SierraBioSystems Inc., Sonoma, CA, USA). RNA synthesis with 3'-dT overhang was prepared on a dT preloaded controlled pore glass (CPG) solid support (30 mg, 1  $\mu$ mol) placed into each RNA synthesis column. RNA phosphoramidites (0.15 M) were dissolved in acetonitrile (MeCN) and placed onto the synthesizer under argon gas ( $\text{Ar}_{(g)}$ ) for coupling (720 sec.) during the RNA synthesis cycle. The automated RNA synthesis cycle consisted of the following steps: (1) Detritylation: MeCN wash followed by addition of 3% trichloroacetic acid (TCA) in DCM. (2) Coupling: delivery of the appropriate amidite coupled with the addition of the activator (0.25 M ethylthiotetrazole (ETT) in MeCN), followed by MeCN wash steps. (3) Capping: Addition of the Cap A reagent (acetic anhydride,  $\text{Ac}_2\text{O}$ , in pyridine, pyr, and tetrahydrofuran, THF), followed by the addition of the Cap B reagent (16% *N*-methyl imidazole, NMI, in THF), with a subsequent MeCN wash steps. (4) Oxidation: delivery of oxidizing solution (0.1 M iodine,  $\text{I}_2$  in 75:20:5 v/v/v pyr,  $\text{H}_2\text{O}$ , THF), followed by MeCN wash steps. This cycle was repeated for the addition of each individual phosphoramidite until the full-length RNA sequence was completed. At the end of the RNA synthesis cycle a final detritylation step removes the 5'-DMT protecting group from the support-bound RNA sequences.

For the branching sequences, an asymmetric branching phosphoramidite (Chemgenes, CLP-1769) was prepared as previously described for RNA phosphoramidites (0.15 M) and placed on the synthesizer. The branchpoint phosphoramidite was then coupled (720 sec.) to the 5'-end of the CPG-bound RNA sequences using the same synthesis cycle outlined above in trityl ON mode to omit the detritylation step of the branchpoint phosphoramidite. The column was then removed from the synthesizer, and subjected to a decyanoethylation reaction converting the phosphate triester to diester form to minimize RNA strand migration and/or cleavage reactions during the subsequent acid detritylation step. This was done by passing a solution of 2:3 v/v triethylamine

(NEt<sub>3</sub>):MeCN dropwise through the column with a syringe for 10 min and then allowing the reaction to complete for 80 min on a shaker. The column was then washed with 50 mL of MeCN and returned to the synthesizer. The next RNA sequence was synthesized using the same RNA synthesis cycle outlined above. The second RNA synthesis was completed by a final detritylation step and subsequent capping of the liberated 5'-OH group to avoid additional reactions at this site.

The column was then removed from the synthesizer and subjected to a delevulination reaction to remove the levulinyl group from the branchpoint phosphoramidite. This was done by passing a solution of 0.5 M hydrazine hydrate (NH<sub>2</sub>NH<sub>2</sub>·H<sub>2</sub>O) in 2:3 v/v acetic acid (AcOH) and pyr, added dropwise through the column for 20 min using a syringe. The column was then washed with 50 mL of MeCN and dried on the synthesizer with Ar<sub>(g)</sub>. The branch V-shaped RNA templates were either used directly or fluorescently labelled at the branchpoint position as outlined in section 1.3. The branch V-shape RNA templates was also extended from the liberated -OH group at the branchpoint position with RNA phosphoramidites (0.15 M MeCN) following the same RNA synthesis protocol to generate the branched Y-shaped RNA templates in trityl-OFF mode that liberated the terminal 5'-OH group.

Following oligonucleotide synthesis, the unlabelled RNA sequences were cleaved from the CPG solid-support and deprotected using 1:1 v/v methylamine:ammonium hydroxide (1 mL of AMA conditions) at room temperature for 20 min. For fluorochrome labelled RNA sequences, it was found that the AMA conditions led to degradation of the respective fluorophore. Modified cleavage and deprotection conditions that were applicable to fluorescently-labelled samples consisted of 2:1:1 v/v/v ammonium hydroxide (NH<sub>4</sub>OH): propylamine:water (1 mL of APA conditions) placed on a heating block set to 65 °C for 45 min. Following cleavage and deprotection, the samples were placed in an Integrated Savant ISS100 SpeedVac concentrator to evaporate the RNA samples to dryness. The crude RNA was extracted from the CPG, in 1 mL of sterile (autoclaved) MilliQ-filtered H<sub>2</sub>O and centrifuged. The supernatant was collected and subsequently analyzed by Ultraviolet-Visible (UV-Vis) spectroscopy for RNA quantitation.

The crude RNA samples were then evaporated to dryness on a SpeedVac concentrator. The dried RNA pellet was redissolved in a mixture of 1:1.25 v/v dimethylsulfoxide:triethylamine trihydrofluoride (DMSO:TREAT-HF, 100 μL:125 μL) to complete the RNA 2'-desilylation

reaction at 65 °C for 90 min. The crude RNA samples were subsequently precipitated from the reaction mixture with 3 M NaOAc (25 µL) in cold n-BuOH (1 mL). Precipitation was completed on ice for 1 h prior to centrifugation (8 000 rpm) leaving the crude RNA samples as a solid white pellet. The RNA samples were redissolved in autoclaved milliQ H<sub>2</sub>O (1 mL) and the crude RNA recoveries were determined by UV absorbance measurements at 260 nm.

### *1.3 Fluorochrome labelling of RNA sequences*

Following V-shape RNA template synthesis, the addition of the monomethoxytrityl (MMT)-amino hexamethylene (C-6) phosphoramidite linker (ChemGenes, CLP-1563) was coupled to the free hydroxyl (-OH) group present at the branchpoint position of the V-shaped RNA template. The RNA synthesis protocol described above was used to couple the amino linker to the RNA sequences. The sample was then subject to three additional detritylation steps to completely remove the MMT protecting group from the amino linker, which was indicated by the absence of the yellow MMT<sup>+</sup> colour following each detritylation step.

For fluorescein isothiocyanate (FITC) labelling, the CPG-bound amino linker modified RNA templates were removed from the synthesizer column and transferred into an Eppendorf tube. The CPG-bound amino linked RNA samples (1 µmol, 40 mg) were then reacted with FITC (15 eq., 15 µmol, 11.7 mg), and *N,N*-diisopropylethylamine (DIEA, 20 eq., 20 µmol, 1.3 µL) dissolved in anhydrous *N,N*-dimethylformamide (DMF, 300 µL) within the Eppendorf tube agitated on a benchtop shaker for 24 h at room temperature in the dark. Following reaction, the CPG was centrifuged, and the supernatant was removed. The CPG was further washed with DMF (3 x 1 mL) and MeCN (3 x 1 mL) until no FITC color remained in the extracted supernatant. The CPG-bound FITC-labelled RNA samples were then cleaved and deprotected using the APA conditions as outlined in section 1.2.

For coumarin (CM)-labelling, the CPG-bound amino linker modified V-shape RNA template was removed from the synthesizer and the CPG was transferred into an Eppendorf tube. The CPG-bound amino linked RNA sample (1 µmol, 40 mg) was then suspended in a mixture of coumarin carboxaldehyde (10 eq., 1.7 mg, 10 µmol) dissolved in tetrahydrofuran (THF, 100 µL, 0.1 M) The reaction was agitated on a benchtop shaker for 2 h at room temperature. The intermediate imine was then reduced by the addition of sodium cyanoborohydride, NaBH<sub>3</sub>CN (5-10 µL, 100 eq., 100 µmol, 0.9 M) in THF and agitated on a benchtop shaker for an additional 6 h

at room temperature. Following the reaction, the CPG was centrifuged, and the supernatant was removed. The CPG was washed with THF (3 x 1 mL) until no coumarin colour remained in the extracted supernatant. The CPG-bound CM-labelled V-shape RNA template was then cleaved and deprotected from CPG solid support using APA conditions as outlined in section 1.2.

#### *1.4 Ultraviolet-Visible (UV-Vis) spectroscopy*

RNA samples dissolved in autoclaved milliQ H<sub>2</sub>O (1 mL) were transferred into quartz cuvette (1 cm pathlength) and placed into an Agilent HP 8453 photodiode array (PDA) UV-Vis spectrophotometer. The UV-Vis spectra were collected from 190-500 nm and corrected against a blank of milliQ H<sub>2</sub>O. Quantitation of RNA content was based on measuring the absorbances at 260 nm. RNA quantitation was initially determined in optical density (O.D.) units, measuring the absorbance units (a.u.) of RNA samples dissolved in (1 mL) H<sub>2</sub>O. The Beer Lambert Law using the molar extinction coefficients  $\epsilon_{\text{nucl.}}$  (M<sup>-1</sup> cm<sup>-1</sup>) associated with the nucleobase content in sequence compositions were used to calculate RNA concentrations in H<sub>2</sub>O (1 mL). The absorbance measurement at 450 nm was used to determine the presence of FITC, and at 310 nm for confirming the presence of CM. The blank-corrected UV-Vis spectral data was exported to Excel and plotted.

#### *1.5 Reversed Phase Ion-Pairing High Performance Liquid Chromatography (RP IP HPLC)*

The crude RNA samples were initially analyzed by RP IP HPLC to assess crude purities. The HPLC analyses (1.0 O.D.) and purifications (20-30 O.D.) were performed on an Agilent 1100 Series HPLC equipped with variable wavelength absorbance detection set at 260 nm. Crude RNA samples were dissolved in autoclaved milliQ H<sub>2</sub>O (1 mL) and syringe filtered (0.22  $\mu\text{m}$ ) into HPLC vials for auto-injection into a Waters<sup>®</sup> XBridge C-18 reverse phase column (4.6 x 250 mm, 5  $\mu\text{m}$ ) heated at 60 °C. HPLC analyses and purifications were conducted using a gradient of 20 or 35-85% eluent B (20% MeCN in 0.1 M triethylammonium acetate, TEAA pH 7.4) in eluent A (0.1 M TEAA, pH 7.4) over a 15-17 min elution period with a HPLC flow rate set at 1 mL/min. Retention times (min) and peak areas (% area) were integrated with ChemStation (Agilent<sup>®</sup>) and used to confirm RNA purities  $\geq 90\%$  following RNA sample purifications.

#### *1.6 Mass Spectrometry (MS)*

Pure RNA samples (0.33-1  $\mu\text{M}$ ) dissolved in milli-Q  $\text{H}_2\text{O}$  (1 mL) were analyzed by Dr. Alexander Wahba at the McGill University Center for Mass Spectrometry, Montreal, QC. Samples were analyzed on a Bruker Maxis Impact Q-TOF ESI LCMS in negative mode. The mass spectral data was obtained and deconvoluted as observed mass/charge ( $m/z$ ) ratios confirming the presence of the RNA sequence molecular ion using the Bruker Compass DataAnalysis 4.2 software. Theoretical masses were calculated by entering each sequence identity on IDT OligoAnalyzer (<https://www.idtdna.com/calc/analyzer>).

### *1.7 RNA hybridization*

Equimolar quantities ( $\sim 1$  nmol) of complementary (antisense, A and sense, S) RNA strands were combined and mixed in either phosphate buffered saline (PBS) (1 mL, 100 mM  $\text{Na}_3\text{PO}_4$ , 150 mM NaCl, 1 mM EDTA, pH 7.5), Tris-HCl (1 mL, Tris-HCl 10 mM, NaCl 50 mM, 1 mM EDTA pH 7.6) or HEPES (1 mL, 100 mM  $\text{KCH}_3\text{COO}$ , 30 mM HEPES, pH 7.5) annealing buffer using sterile, autoclaved milli-Q filtered  $\text{H}_2\text{O}$  and then syringe filtered (0.22  $\mu\text{m}$ ) in separate microtubes and annealed to produce hybrid double-stranded (ds) RNA duplex structures that templates the self-assembly of higher-ordered (nano)structures (ex. nanosquares, nanocubes and nanotube shaped RNA). In the annealing/hybridization process, the RNA samples were placed on a heating block at 95  $^\circ\text{C}$  for 5 min to initially denature higher-ordered structures or self-folding interactions. The RNA samples were then slowly cooled to room temperature for 3 h and subsequently stored at 4  $^\circ\text{C}$  overnight to favor hybrid duplex formation and assembly of stable, discrete RNA nanostructures.

### *1.8 Denaturing Polyacrylamide Gel Electrophoresis (PAGE)*

Single-stranded RNA samples were initially analyzed and characterized on a denaturing (7M urea) PAGE. The RNA samples were aliquoted ( $\sim 0.3$  O.D) into separate Eppendorf tubes and evaporated on a SpeedVac concentrator. The solid RNA samples were then redissolved in a denaturing formamide gel loading buffer (30  $\mu\text{L}$ , 4:1 v/v formamide: 10X TBE, tris(hydroxymethyl)aminomethane (TRIS) (54.5 g), boric acid (27.8 g) and ethylenediaminetetracetic acid (EDTA) (1.86 g) in milliQ  $\text{H}_2\text{O}$  (500 mL), pH 8). The samples were then loaded into a 20% denaturing PAGE (7 M urea (21 g), 20% acrylamide gel (40% acrylamide and  $N,N$ -methylene bisacrylamide 19:1 v/v solution, 25 mL), prepared using 10x TBE buffer solution (5 mL) polymerized with ammonium persulfate (APS, 350 mL) and  $N,N,N',N'$ -

tetramethylethylenediamine (TEMED, 15  $\mu$ L). The denaturing PAGE was run in 1X TBE running gel buffer at 250V for 20 min. and then increased to 300V for 3-4 h. A tracking dye (xylene cyanol, XC and bromophenol blue, BPB in formamide gel loading buffer, 30 mL) was used to track the duration of the PAGE. An oligonucleotide length ladder (IDT™, 20-100 oligo length standards) formulated in formamide gel loading buffer (1:1 v/v, 30 mL) was used for the characterization of various-length RNA samples. Gels were visualized under short (RNA detection at 254 nm) and long (FITC detection at 450 nm) range UV-shadowing and subsequently placed in a Stains-All® (Sigma) solution (25 mg Stains-All®, 50 mL isopropyl alcohol, 25 mL formamide, 125 mL water). After overnight treatment, the gel was removed from the stain solution and exposed to light to destain and visualize the stained oligonucleotide bands.

### *1.9 Native PAGE*

Single-stranded (~0.3 O.D. of ssRNA) and the double-stranded hybrid RNA samples were prepared by aliquoting stoichiometric quantities (1 nmol) of complementary ssRNA (~0.3 – 0.5 OD total RNA content). Hybrid RNA samples were annealed in PBS (10  $\mu$ L, 0.25 – 0.75 nmol dsRNA) as outlined in section 1.7. Following sample hybridization, the native, non-denaturing glycerol gel loading buffer (20  $\mu$ L, 30% glycerol in 10X TBE, pH 8) was then added to each RNA sample for PAGE analysis. The RNA samples were then loaded into a 16% non-denaturing native PAGE in 1X TBE running gel buffer at 250 V for 20 min and then increased to 300 V for 3-4 h. A tracking dye (xylene cyanol, XC, and bromophenol blue, BPB, in formamide gel loading buffer, 30 mL) was used to track the migration of the oligonucleotides and duration of the PAGE. A double-stranded base-pair (bp) oligonucleotide length ladder (NEB™, 25 bp to 766 bp standards) formulated in glycerol gel loading buffer (1:1 v/v, 30 mL) was used for the characterization of hybrid RNA samples. Gels were visualized under short (RNA detection at 254 nm) and long (FITC detection at 450 nm) range UV-shadowing and subsequently placed in a Stains-All® (Sigma) solution to visualize the stained oligonucleotide bands.

### *1.10 Circular dichroism (CD) spectroscopy*

RNA hybrid samples were prepared in equimolar (1 nmol) quantities in PBS annealing buffer or in milli-Q H<sub>2</sub>O (1 mL, 1  $\mu$ M) as described in section 1.7. The samples were then placed into a black cell quartz cuvette (300  $\mu$ L, 1 cm path length) and analyzed in a Jasco J-815-150S circular dichroism (CD) spectrometer. The CD spectrometer was initially purged with N<sub>2</sub> for 20

min. Samples were run in triplicate measurements and spectral data was averaged and corrected against a blank (buffer or H<sub>2</sub>O) spectrum. Scans were collected with 1 nm bandwidth interval, 0.5 nm sampling interval over a range of 200-300 nm. Data was smoothed, exported and plotted in Microsoft Excel as changes in molar ellipticity ( $\theta$ ) with increasing wavelengths (210 – 310 nm).

### *1.11 Thermal denaturation ( $T_m$ )*

RNA hybrid duplexes were prepared in equimolar (1 nmol) quantities in PBS annealing buffer or milli-Q H<sub>2</sub>O (1 mL, 1  $\mu$ M) as outlined in section 1.7. The samples were then added into 1 mL quartz cuvettes (1 cm path length) and placed into a Cary 100 UV-Vis spectrophotometer equipped with a Peltier multicell temperature controller for thermal denaturation ( $T_m$ ) measurements. The instrument was initially purged with nitrogen gas (N<sub>2(g)</sub>) for 5 min. The melting curves were collected at a wavelength of 260 nm over a temperature range of 25 – 90 °C, with a scanning rate set at 5 °C/min. Data was exported to Excel and plotted as changes in percent (%) hyperchromicity observed at 260 nm against changes in temperature (25-90 °C). The melting temperature ( $T_m$ ) was calculated from the first derivative plots of the melting curves, representing the temperature at which 50% of the duplex denatured into single stranded RNA.

### *1.12 Fluorescence spectroscopy*

The RNA hybrid samples with FITC alone, or CM alone, or in combination (FITC+CM) with both fluorophores (to examine FRET pair signaling) were used to determine the fluorescence excitation and emission spectra. RNA hybrid samples were prepared in equimolar quantities in PBS annealing buffer (1  $\mu$ M, 1 mL), as previously described in section 1.7. As controls, the FITC and coumarin labelled single stranded (ss)RNA samples were also prepared in PBS annealing buffer (1 mL, 1  $\mu$ M). UV-Vis absorbance spectra of the fluorophore-labelled RNA hybrid samples was first collected on an Agilent HP 8453 Photodiode Array (PDA) spectrophotometer between 190–500 nm to confirm the FITC and CM absorbance and excitation wavelengths ( $\lambda$ ). Fluorescence excitation and emission spectra were obtained on a Perkin Elmer LS 55 luminescence spectrophotometer from 250-600 nm with the excitation and emission wavelengths set to:  $\lambda_{\text{ex, FITC}} = 492$  nm,  $\lambda_{\text{ex, coumarin}} = 320$  nm;  $\lambda_{\text{em, FITC}} = 520$  nm,  $\lambda_{\text{em, coumarin}} = 420$  nm. The spectral data was background corrected with PBS annealing buffer and exported into Microsoft Excel and plotted as fluorescence intensity (F.I.) against the wavelength (nm).

### *1.13 Transmission Electron Microscopy (TEM) and Energy Dispersive X-ray (EDX) spectroscopy*

RNA hybrid samples (1  $\mu\text{M}$ , 1 mL) were hybridized in either sterile milliQ  $\text{H}_2\text{O}$  or PBS annealing buffer as previously described. An aliquot (3  $\mu\text{L}$ ) of the RNA samples was placed on a 300-mesh copper grid coated with a carbon thin-film (Electron Microscopy Sciences Inc., Hatfield, PA.). The RNA sample was left to adsorb on the grid for 60 s and dabbed with the edge of a Kimwipe to remove excess  $\text{H}_2\text{O}$ . An aliquot of milliQ  $\text{H}_2\text{O}$  (3  $\mu\text{L}$ ) was then placed onto the sample and let sit for 10 s before drying with a Kimwipe as previously described. An equal volume amount (3  $\mu\text{L}$ ) of a 1% uranyl acetate aqueous solution was then placed onto the RNA sample and allowed to adsorb on the copper grid for 10 s and subsequently dabbed with the edge of a Kimwipe to remove the excess liquid. This cycle was repeated twice to ensure optimal sample adsorption onto the copper grids. TEM images were obtained using a FEI Tecnai G2 F20 Transmission Microscope at an accelerating voltage of 120 kV and the Gatan ORIUS TEM CCD Camera was used to capture images across the grids. The Oxford X-Max 80  $\text{mm}^2$  Energy Dispersive X-ray (EDX) detector was used with the Aztec software for EDX analysis. Particle size measurements of the observed widths (nm) and lengths (nm) were taken using ImageJ software (LOCI, University of Wisconsin). Average mean measurement values and their standard deviations were calculated and reported.

### *1.14 Dynamic Light Scattering (DLS) and zeta potential measurements*

RNA hybrid samples in either sterile, milliQ  $\text{H}_2\text{O}$  or PBS annealing buffer (1  $\mu\text{M}$ , 1 mL) were prepared as outlined previously described. The RNA samples were then transferred into a 1 mL cuvette (1 cm pathlength) and placed into Brookhaven NanoBrook Omni dynamic light scattering (DLS) instrument. The RNA samples were analyzed at 25  $^\circ\text{C}$  with a 30 s acquisition time for the collection of 10 replicate measurements. The laser intensity was adjusted to a count rate between 1000 – 5000. From the sample cuvette, an aliquot (700  $\mu\text{L}$ ) was then removed and an electrode probe used for zeta-potential measurements was connected to the DLS instrument and inserted into the sample solution. Zeta potentials were recorded using the Particle Solutions v.3.6.0.7136 software with a protocol of 20 cycles that collected 20 measurements over an acquisition time of 2 min. Particle size and zeta potential measurements were reported as average mean values with standard deviations.

### *1.15 Atomic Force Microscopy (AFM)*

Mica sheets for sample imaging were purchased from Ted Pella, Inc (Redding, CA, USA). The surface of mica plates was cleaved using an adhesive tape. siRNA samples were annealed in H<sub>2</sub>O as described in section 1.7, the day prior to sample deposition on mica surfaces. To reduce sample aggregation, the samples were filtered through 0.22 μm syringe filters prior to hybridization. Following cleavage, 10 μL of 1 μM (square) or 100 nM (Cube, Tube) samples were added to the mica surface and allowed to adhere and dry for 1-4 days prior to AFM analysis. The AFM images were acquired in tapping mode in air using a NT-MDT Ntegra AFM system equipped with 0.35 N/m Bruker silicon probes operating at 67 kHz and having a 10 nm radius tip. Particle size measurements and image processing were conducted using the Nova software.

### *1.16 Raman microspectroscopy*

The A549 cells were seeded onto #1.5H glass coverslips pre-coated with poly-D-lysine at a density of  $3.5 \times 10^5$  cells per 35 mm dish and cultured for 24 h. Cells were then transfected with siRNA samples (cube, tube, or square configurations) for 4 h. Following transfection, cells were fixed with formalin at room temperature for 15–30 min. To eliminate Raman interference from media components and salts, the fixative was removed, and the samples were gently rinsed three times with 2 mL of milli-Q H<sub>2</sub>O, with each wash step lasting 3 min. After the final rinse, the water was aspirated, and the coverslips were allowed to air-dry completely at room temperature for approximately 2 h. The dried samples were stored in a multi-well plate lined with lint-free wipes (Kimwipes) with the cell-side facing upward until Raman analysis was performed.

Chemical composition of the samples (“cube”, “square”, “tube”) were characterized using a confocal Raman microscope (alpha300, WITec GmbH, Germany) equipped with a UHTS300S spectrometer and a DU401-BVF CCD detector. A 532.2 nm excitation laser operating at 20 mW was used with a Zeiss EC Epiplan-Neofluar 100x objective. For each sample, 3 spectra were collected with an integration time of 5 s and 5 averages. Spectra were collected over the 0-3500 cm<sup>-1</sup> range using a 600 g/mm diffraction grating centered at 597.39 nm. For whole-cell measurements (“cube” and “tube”), Raman hyperspectral maps were acquired using large-area scanning. Area scans covered regions of 28 × 62 μm with a spatial resolution of 56 × 124 pixels (total 6944 spectra per map). Each spectrum was collected with a 2.5 s integration, resulting in a total acquisition time of approximately 5 h per map. Samples were subsequently analyzed using

WITec Project Plus 7 (WITec GmbH, Germany). Raman hyperspectral datasets were processed using True Component Analysis (TCA) to identify chemically distinct spectral components within the mapped regions. The extracted components were compared against reference spectra obtained from the corresponding sample materials to assist in spectral assignment and chemical interpretation. Prior to analysis, spectra were cosmic-ray corrected and baseline corrected using the standard software routines.

### *1.17 Cell Culture*

The human lung adenocarcinoma A549 cells (ATCC® CCL-185™) were grown in Dulbecco's Modified Eagle's Medium (DMEM; Corning 10-013-CV) supplemented with 10% FBS, 4.5 g/L glucose, L-glutamine, and sodium pyruvate and incubated at 37°C, in a ThermoForma triple gas (N<sub>2</sub>-O<sub>2</sub>-CO<sub>2</sub>) incubator set at 21% O<sub>2</sub> and 5% CO<sub>2</sub>, with 95% relative humidity. All cell work was conducted in a biosafety cabinet (ThermoFisher Scientific – 1300 Series A2 Hood).

### *1.18 siRNA Transfections*

Briefly, the A549 cancer cells ( $3 \times 10^5$ ) were plated in 6-well culture plates containing DMEM culture media with 10% FBS and were incubated for 24 h in a humidified incubator set at 37 °C with 5% CO<sub>2</sub>. Prior to transfections, the siRNA hybrids (10 µL, 5 µM, in 1X Opti-MEM, 250 µL) were mixed with the transfection reagents (Lipofectamine 3000™, 6 µL in Opti-MEM, 250 µL) according to the manufacture's recommendation. The mixtures were incubated (15 min, room temperature) then added to the A549 cell culture at a final siRNA treatment concentration of 25 nM. The cell culture was incubated at 37 °C with 5% CO<sub>2</sub> over 66 h for RT-qPCR and western blot analyses. Cell proliferation (confluency) over time (66 h) was monitored as an indicator of cell viability in an Incucyte™ (Essen BioScience).

### *1.19 Flow cytometry*

The A549 cells were detached from a T-75 cm flask using 1X trypsin (1 mL, 3 min), followed by addition of DMEM (4 mL) supplemented with 10% FBS. The cells were collected in a 15 mL canonical tube, and spun down in a (MIKRO 220 Hettich) centrifuge at 1500 RPM for 5 min. The cell pellet was washed twice with serum free DMEM to remove FBS. Finally, the cells were suspended in serum free DMEM (4 mL), and analyzed for cell counting, and viability by Trypan Blue (Millipore Sigma; T8154) staining and visualized under a Zeiss Axiovert 200

brightfield microscope at 10X magnification. The A549 cells ( $\sim 5 \times 10^5$ ) were added to microcentrifuge tubes, followed by addition of FITC-labelled siRNA square (25 nM in PBS) with and without Lipofectamine 3000™ (6  $\mu$ L). Samples were incubated for 1 h at 37 °C by rotating and the cells were then washed using 1X PBS, centrifuged at 1,300 rpm and resuspended in PBS for flow cytometry analysis on the BD Accuri C6 flow cytometer with FITC channel detection at 451 nm.

### *1.20 Confocal Fluorescence Microscopy*

Glass coverslips (ThermoFisher, 22x22mm) were sterilized with ethyl alcohol and coated with 1X poly-D-lysine (Millipore Sigma) and incubated at 37 °C for 15 min. The poly-D-lysine was then collected, and the slides were washed three times with 1X PBS, then dried for 1 h under UV light. A549 cells were then counted and seeded at a density of  $3 \times 10^5$  cells per 35 cm plate for 24 h. FITC-labelled siRNA square sample (25 nM) with and without Lipofectamine 3000™ (6  $\mu$ L) was prepared and incubated with the cells in OPTIMEM for 4 h at 37 °C, 5% CO<sub>2</sub>. All proceeding incubations were done at room temperature and washes were conducted using 1X PBS. The cells were washed twice and fixed with 750  $\mu$ L of 4% (MeOH free) formaldehyde (ThermoFisher 28908) in 1X PBS for 15 min. This was followed by two additional washes and cell permeabilization with 1ml of 0.5% Triton X-100 (BioShop) in 1X PBS for 5 min. After two washes, Alexa Fluor™ 647 phalloidin (ThermoFisher A22287) was diluted 400X in 1X PBS. 1 mL of this solution was added and incubated for 15 min in the dark prior to performing three final washes. The cells were inverted onto a 1.5 mm microscope slide with a drop of (Globe Scientific slides 25mm x 75mm x 1mm Item#: 1304W) Fluoroshield with DAPI mounting media (Millipore Sigma; F6057) and imaged by confocal microscopy.

For colocalization studies, the A549 cells were seeded onto  $\mu$ -slide 8 well İbidi plates (cat no:80826) at a cell density of  $1 \times 10^4$  cells/well and cultured in EMEM supplemented with 10% FBS for 24 h. Cells were transfected with FITC-square siRNA sample (25 nM) in EMEM (200  $\mu$ L), supplemented with 10% FBS media using Lipofectamine™ 3000 (0.5  $\mu$ L, Invitrogen). At select time points, 1 h and 4 h post transfection, LysoTracker™ Deep Red (ThermoFisher L12492) was added at a final concentration of 1  $\mu$ M and incubated for 30 min. Following a PBS wash and media replenishment, nuclei were stained using NucBlue™ Live Cell Stain (ReadyProbes™, Invitrogen) for 15 min and imaged by confocal microscopy.

Sample images were collected using a laser scanning confocal microscope (LSM 980, Zeiss, Germany) equipped with a 63x/1.40 NA oil immersion objective. Fluorescence excitation was performed using lasers at 405 nm, 488 nm, and 639 nm. Emission signals were detected using GaAsP PMT with spectral detection windows set to 409–471 nm (blue), 489–604 nm (green), and 640–693 nm (red channel). Images were acquired using frame scan mode with a pixel dwell time of 2.64  $\mu$ s. Detector gain was set to 650 V for fluorescence channels. All images were collected using identical acquisition settings to allow quantitative comparison. Colocalization of the FITC-siRNA signal with lysosomes was quantified with Huygens version 25.10 using the "Standard" strategy (Scientific Volume Imaging, The Netherlands) with the Colocalization Analyzer. Images were acquired using identical microscope settings across conditions (laser power, detector gain/offset, pinhole, pixel size) and analyzed using the same processing parameters for all samples. Widefield fluorescence images were acquired on an upright microscope (AxioPlan 2 Imaging, Carl Zeiss) equipped with a 63 $\times$ /1.4 NA oil-immersion objective and mercury arc lamp for fluorescence. Images were acquired using a cooled monochrome CCD camera (QImaging, Canada) with AxioVision 4.8 and QICam. Fluorescence collected using filter sets (Filterset 02, Filterset 17, Filterset 64HE). For each fluorophore/channel, exposure times were adjusted to maximize signal while avoiding pixel saturation and then kept constant across samples within an experiment. Images were saved as 8-bit TIFF files. Where indicated, background images acquired from control cells (no staining) regions using identical acquisition settings were used for background subtraction during image processing.

### *1.21 Fluorescence microscopy*

Glass coverslips (ThermoFisher, 22  $\times$  22 mm) were sterilized with ethyl alcohol and coated with 1 $\times$  poly-D-lysine (Millipore Sigma) and incubated at 37 $^{\circ}$ C for 15 min. The poly-D-lysine was then collected, and the slides were washed three times with 1 $\times$  PBS, then dried for 1 h under UV light. The A545 cells were then counted and seeded at a density of  $3.5 \times 10^5$  cells per 35 cm plate for 24 h. This was followed by transfection with 50 nM of fluorochrome-labelled siRNAs, FITC-square, CM-square and FITC+CM samples in EMEM (10% FBS) using Lipofectamine 3000 (7  $\mu$ L) for 4 h. Cells were washed twice with 1 $\times$  PBS, and then fixed with 4% paraformaldehyde for 10 min, then washed again twice with 1X PBS. To allow for intracellular labeling, cells were permeabilized with 0.1% Triton X-100 in PBS for 5 min, followed by two PBS washes. F-actin

filaments were stained using Alexa Fluor™ 647-conjugated Phalloidin (Invitrogen; 1:400 dilution) for 15 min at room temperature. After a final PBS rinse, coverslips were inverted and mounted onto 1.5 mm microscope slides (Globe Scientific) using Vectashield mounting medium without DAPI (Vector Laboratories). Widefield images were acquired on an inverted microscope IX85 (Evident Scientific) using a 40×/0.60 NA air objective and an X-Cite XYLIS II, Excelitas Technologies for epifluorescence excitation. Images were captured with a DP75 color camera (Evident Scientific). Fluorescence was collected using chroma filter sets (49000, 49002, 49006). For fluorescence imaging, acquisition settings (illumination intensity and exposure time) were selected to avoid saturation and were held constant across comparable samples within an experiment. Images were exported as 8-bit VSI. If fluorescence channels were analyzed quantitatively, images were single-channel grayscale representations per filter, imported to FIJI/ImageJ2, background subtracted, ROIs were selected and area was measured with the total intensity, for further analysis. Widefield representative images were deconvolved with Huygens Professional version 25.10 using the "Standard" strategy (Scientific Volume Imaging, The Netherlands, <http://svi.nl>).

### *1.22 RNA isolation and quantitative RT-PCR*

Grp mRNA was isolated from the A549 cancer cell lines using the manufacturer's protocol (Aurum® Total RNA Mini Kit, BioRad 7326820). The total mRNA levels were quantitated by measuring the absorbance of collected RNA samples at 260 nm using a DeNovix DS-11 spectrophotometer. The isolated RNA (500 ng of each sample) was treated with RNase-free DNase I at room temperature to eliminate residual genomic DNA. These samples were then subjected to reverse-transcription using iScript Reverse Transcriptase and iScript reaction mix according to the manufacturer's protocol (Bio-Rad 1708890). The resulting complementary cDNA was quantified. Each qPCR reaction contained 100 ng of cDNA template, 10 µl of SsoAdvanced Universal SYBR Green Supermix (Bio-Rad 1725270), and 500 nM of forward and reverse primers in a final reaction volume of 20 µl. For human Grp78, the primer sequences were 5'-ACCTCCAACCCCGAGAACA-3' (forward) and 5'-TTCAACCACCTTGAACGGC-3' (reverse). For human Grp94, 5'-ACTGTTGAGGAGCCCATGGAGG-3' (forward) and 5'-GCTGAAGAGTCTCGCGGGAAAC-3' (reverse). For human Grp75, 5'-AGCTGGAATGGCCTTAGTCAT-3' (forward) and 5'-CAGGAGTTGGTAGTACCCAAATC-

3' (reverse). For human Grp170, 5'-CTTCAACCTGGATGAGAGTGGC-3' (forward) and 5'-ACAGGCTGGAAATGGTGTGCC-3' (reverse). For Gapdh, the primer sequences were 5'-ACCACAGTCCATGCCATCAC-3' (forward) and 5'-TCCACCACCCTGTTGCTGTA-3' (reverse). The reactions were carried out using the Bio-Rad CFX Connect Real-Time PCR Detection system for 40 cycles (90 °C for 15 sec, 60 °C for 30 sec). The fold change in the expression of each gene was calculated using the Livak ( $2^{-\Delta\Delta C_t}$ ) method, with Gapdh used as an internal housekeeping gene control for normalization and quantitation of mRNA transcript levels.

### *1.23 Protein isolation and western blots*

The cell media was aspirated from the transfected culture and washed with PBS buffer for 2 min, twice. The cells were lysed on ice using chilled RIPA buffer. Protein concentration of cell lysates was determined using the bovine serum albumin (BSA) protein assay reagent (ThermoFisher Scientific Inc.). Proteins samples (20 µg, 20 µL) were dissolved in 2X Laemmli loading buffer (Biorad), boiled for 5 min, and resolved in 8% and 10% sodium dodecyl sulfate polyacrylamide gel electrophoresis (SDS-PAGE). The proteins were electrotransferred onto a polyvinylidene difluoride membrane (PVDF, Bio-Rad Laboratories), which was blocked in Tris-buffered saline, pH 8.0, Tween-20, 5% (w/v) skimmed milk (TBST solution) for 1 h at room temperature (22 °C). Membranes were then probed with the indicated primary monoclonal antibodies (anti-GRP75, Proteintech, cat. # 67563-1-IG-20UL; anti-GRP78, ThermoFisher, HSPA5 clone 1D6F7; cat. # 66574-1-IG; anti-GRP94, Proteintech, cat. # 60012-2-IG-20UL; anti-GRP170, HYOU1 clone 6F7, Abnova, cat. # H00010525-M01; anti-GAPDH, ABclonal, cat. # A19056) in TBST solution at 4 °C overnight. The next day the membranes were washed with TBST solution (5X, 3 min each) and incubated with an anti-mouse horseradish peroxidase (HRP) conjugated secondary antibody (1:5000) in 5% milk in 1× TBST at room temperature for 1 h followed by washing with TBST solution (5X, 3 min each). Immunoblotted protein bands were visualized by Clarity Western ECL substrate Chemiluminescence (BioRad) mixture (1:1 v/v) and imaged on the Bio-Rad ChemiDock station to visualize the proteins. ImageLab software was used for further analysis of all western blots including protein band densitometry to determine equal protein loading using GAPDH as control housekeeping protein used to normalize and quantitate protein levels of expression.

### *1.24 Cell viability*

The A549 cells were plated at a density of  $4 \times 10^3$  cells per well in a 96-well plate and allowed to incubate for 24 h. The siRNA samples (25 nM, square, cube and tube) were transfected using the Lipofectamine™ 3000 transfection reagent. The A549 cells were incubated for 44 h prior to removing the media and adding resazurin sodium salt (200  $\mu$ L, 60  $\mu$ M) in full serum DMEM. The cells were incubated for an additional 4 h and the absorbance was read at 570 nm and 600 nm on a plate reader. Relative cellular viability to the non-treatment control was calculated and plotted as a function of mean cell viability  $\pm$  SEM for 5 technical replicates.

### *1.25 Statistical Analysis*

Statistical analysis was performed using GraphPad Prism. The error bars for data collection of biological replicates greater than 1, and representative of at least 3 separate experiments (unless otherwise stated), indicates the standard error about the mean values. Statistical significance of relative gene expression (RT-qPCR), confluency (Incucyte™), and cellular toxicity data was determined using an ordinary one-way ANOVA analysis with Dunnett's post hoc for multiple comparisons. Graphical statistical significance indicators are presented based on the Dunnett's post hoc analysis in the graphpad (\* $p < 0.05$ , \*\* $p < 0.01$ , \*\*\* $p < 0.001$ , \*\*\*\* $p < 0.0001$ ) format. Colocalization data was quantified in the FITC and the LysoTracker channels using Manders coefficients (M1 and M2) and the Pearson correlation coefficient. Values displayed as individual data points with mean  $\pm$  SD. Statistical comparisons between 1 h and 4 h were performed using a two-tailed test (unpaired), with significance defined at \* $p < 0.05$ . Statistical analysis of the normalized differences in mean fluorescence intensity (MFI) values plotted as mean MFI  $\pm$  SEM for FITC and LysoTracker at 1 and 4 h were based on the ANOVA significance analysis that included the control data, which was normalized to Tukey's post hoc for multiple comparisons, with significance of \*\* $p < 0.01$ .

**Table S1.** GRP-silencing RNA Antisense (A) and Sense (S) sequences

<b>AGRP75</b>	5' – UUG UAU UCU CCG AGU CAG U –3'
<b>SGRP75</b>	5' – ACU GAC UCG GAG AAU ACA A –3'
<b>AGRP78</b>	5' – AUC AGA AUC UUC CAA CAC U –3'
<b>SGRP78</b>	5' – AGU GUU GGA AGA UUC UGA U –3'
<b>AGRP94</b>	5' – GGU AAU CAG AUG CUU CUU C –3'
<b>SGRP94</b>	5' – GAA GAA GCA UCU GAU UAC C –3'
<b>AGRP170</b>	5' – GCU CAA UAA GGC CAA GUU U –3'
<b>SGRP170</b>	5' – AAA CUU GGC CUU AUU GAG C –3'

**Table S2.** Characterization data of the RNA sequences used in this study

	Template Sequence	%Purity	Theoretical Mass (Da)	Experimental Mass (Da)	Purified Quantity (OD/mL)	Purified Quantity (nmol/ $\mu$ M)	Extinction coefficient at 260 nm ( $M^{-1}cm^{-1}$ )
<b>Controls</b>	LA75 (20-mer ctrl)	>99%	6,282.70	6,277.70	85	432.1	196700
	LA75A78 (39-mer ctrl)	>99%	12,294.26	12,330.29	117	303.8	385100
	LA75A78A94 (58-mer ctrl)	>99%	18,355.79	18,430.71	118	206.8	570600
<b>Square</b>	1 VA75A78	>95%	12,474.26	12,484.01	5.76	15.11	381200
	2 VS75A170	>95%	12,685.51	12,734.20	6.30	15.70	400000
	3 VS94S170	>95%	12,693.43	12,611.49	7.31	18.28	399800
	4 VA94S78	>95%	12,651.34	12,660.73	7.23	18.01	401300
	1-F VA75A78-FITC	>95%	13,086.92	13,052.06	1.19	3.12	381200
	2-CM VS75A170-CM	>90%	12,845.77	12,642.46	2.78	6.93	401300
<b>Cube</b>	1 YA75A75A75	>90%	18,553.37	18,511.68	5.74	10.06	570300
	2 YA170A94S75	>90%	18,761.20	18,451.85	7.83	13.36	586300
	3 YS170A78S75	>90%	18,688.19	18,683.93	2.41	4.14	582300
	4 YS75S78S94	>90%	18,888.33	18,884.45	2.74	7.95	608500
<b>Tube</b>	1 YA75A78A94	>90%	18,549.94	18,507.42	5.08	8.96	567200
	2 YS75S78S94	>90%	18,888.33	18,884.83	5.47	8.99	608500

**Table S3.** List of forward and reverse primer sequences used for RT qPCR.

Primers	Forward sequence	Reverse sequence
Gapdh	5'-ACCACAGTCCATGCCATCAC-3'	5'-TCCACCACCCTGTTGCTGTA-3'
Grp78	5'-ACCTCCAACCCCGAGAACA-3'	5'-TTCAACCACCTTGAACGGC-3'
Grp75	5'-AGCTGGAATGGCCTTAGTCAT-3'	5'-CAGGAGTTGGTAGTACCCAAATC-3'
Grp94	5'-ACTGTTGAGGAGCCCATGGAGG-3'	5'-GCTGAAGAGTCTCGCGGGAAAC-3'
Grp170	5'-CTTCAACCTGGATGAGAGTGGC-3'	5'-ACAGGCTGGAAATGGTGTGTC-3'

**Table S4.** NCBI BLAST (blastn) against the human RefSeq RNA database to screen mRNA transcript (sense-strand) on-target specificity and off-target transcripts against each antisense strand in the GRP-targeting siRNA sequences.

Top (five) ranked candidates shown. E-values approaching 0 demonstrate complete on-target sequence specificity, whereas E-values approaching and exceeding 1 indicates off-target sequences with negligible specificity.

A. GRP75; HSPA9 heat shock protein family A (Hsp70) member 9 gene (mRNA) transcript

Description of Gene Target	Accession #	Query Cover	E value	% Ident.
1. Homosapiens heat shock protein family A (Hsp70) member 9 (HSPA9), mRNA	NM_004134.7	95%	0.04	100%
2. Homosapiens ubiquitin protein ligase E3 component n recognin 1 (UBR1), mRNA	NM_174916.3	74%	9.7	100%
3. Homo sapiens FHF complex subunit HOOK interacting protein 1A (FH1P1A), mRNA	XM_054350782.1	68%	38	100%
4. Homo sapiens amino adipate aminotransferase (ADAT), mRNA	XM_006714231.3	68%	38	100%
5. Homo sapiens EMAP like 6 (EML6), transcript variant X7, mRNA	XM_017004101.2	68%	38	100%

B. GRP78; HSPA5 heat shock protein family A (Hsp70) member 5 gene (mRNA) transcript

Description of Gene Target	Accession #	Query Cover	E value	% Ident.
1. Homosapiens heat shock protein family A (Hsp70) member 5 (HSPA5), mRNA	NM_005347.5	100%	0.01	100%
2. Homosapiens Morf4 family associated protein 1 like 1 (MRFAP1L1), mRNA	NM_203462.3	100%	0.62	100%
3. Homo sapiens tuftelin interacting protein 11 (TFIP11), transcript variant 5, mRNA	NM_001346859.2	100%	0.62	100%
4. Homo sapiens tuftelin interacting protein 11	NM_001246857.2	100%	0.62	100%

(TFIP11), transcript variant 3, mRNA				
5. Homo sapiens tuftelin interacting protein 11 (TFIP11), transcript variant 4, mRNA	NM_001246858.2	100%	0.62	100%

C. GRP94; HSP90B1 heat shock protein 90 beta family member 1 (Hsp90B1) gene (mRNA) transcript

Description of Gene Target	Accession #	Query Cover	E value	% Ident.
1. Homosapiens heat shock protein 90 beta family member 1 (Hsp90B1), mRNA	NM003299.3	100%	0.01	100%
2. Homosapiens B-Raf proto-oncogene, serine/threonine kinase (BRAF), transcript variant 8, mRNA	NM_001378469.1	79%	2.40	100%
3. Homosapiens B-Raf proto-oncogene, serine/threonine kinase (BRAF), transcript variant 12, mRNA	NM_001378473.1	79%	2.40	100%
4. Homosapiens B-Raf proto-oncogene, serine/threonine kinase (BRAF), transcript variant 4, mRNA	NM_001374244.1	79%	2.40	100%
5. Homo sapiens LOC124901146, transcript variant X2, ncRNA	XR_007076183.1	79%	2.40	100%

D. GRP170; HYOU1 hypoxia upregulated 1 (Hyou1) gene (mRNA) transcript

Description of Gene Target	Accession #	Query Cover	E value	% Ident.
1. Homosapiens hypoxia upregulated 1 (HYOU1), transcript variant X6, mRNA	XM_047426254.1	100%	0.01	100%
2. Homosapiens hypoxia upregulated 1 (HYOU1), transcript variant X1, mRNA	XM_005271392.5	100%	0.01	100%
3. Homosapiens hypoxia upregulated 1 (HYOU1), transcript variant X3, mRNA	XM_054367472.1	100%	0.01	100%
4. Homosapiens hypoxia upregulated 1 (HYOU1), transcript variant X2, mRNA	XM_054331612.1	100%	0.01	100%
5. Homosapiens hypoxia upregulated 1 (HYOU1), transcript variant X3, mRNA	XM_005271394.4	100%	0.01	100%

**Table S5.** Size and height measurements of the RNA nanostructures by AFM. Data representative of the mean values of 10 individual measurements per sample  $\pm$  Std. dev.

Sample	Size (nm)	Height (nm)
I. Square (single particles)	55.86 $\pm$ 5.76	28.85 $\pm$ 2.72
II. Cube (single particles)	59.69 $\pm$ 5.58	3.09 $\pm$ 0.78
Cube (partial aggregated cluster)	53.89 $\pm$ 6.89	9.79 $\pm$ 0.39
Cube (full aggregated cluster)	152.54 $\pm$ 20.56	10.17 $\pm$ 0.62
III. Tube (fibril widths)	177.75 $\pm$ 22.30	31.05 $\pm$ 3.91
Tube (single particles)	96.48 $\pm$ 2.68	30.60 $\pm$ 4.35

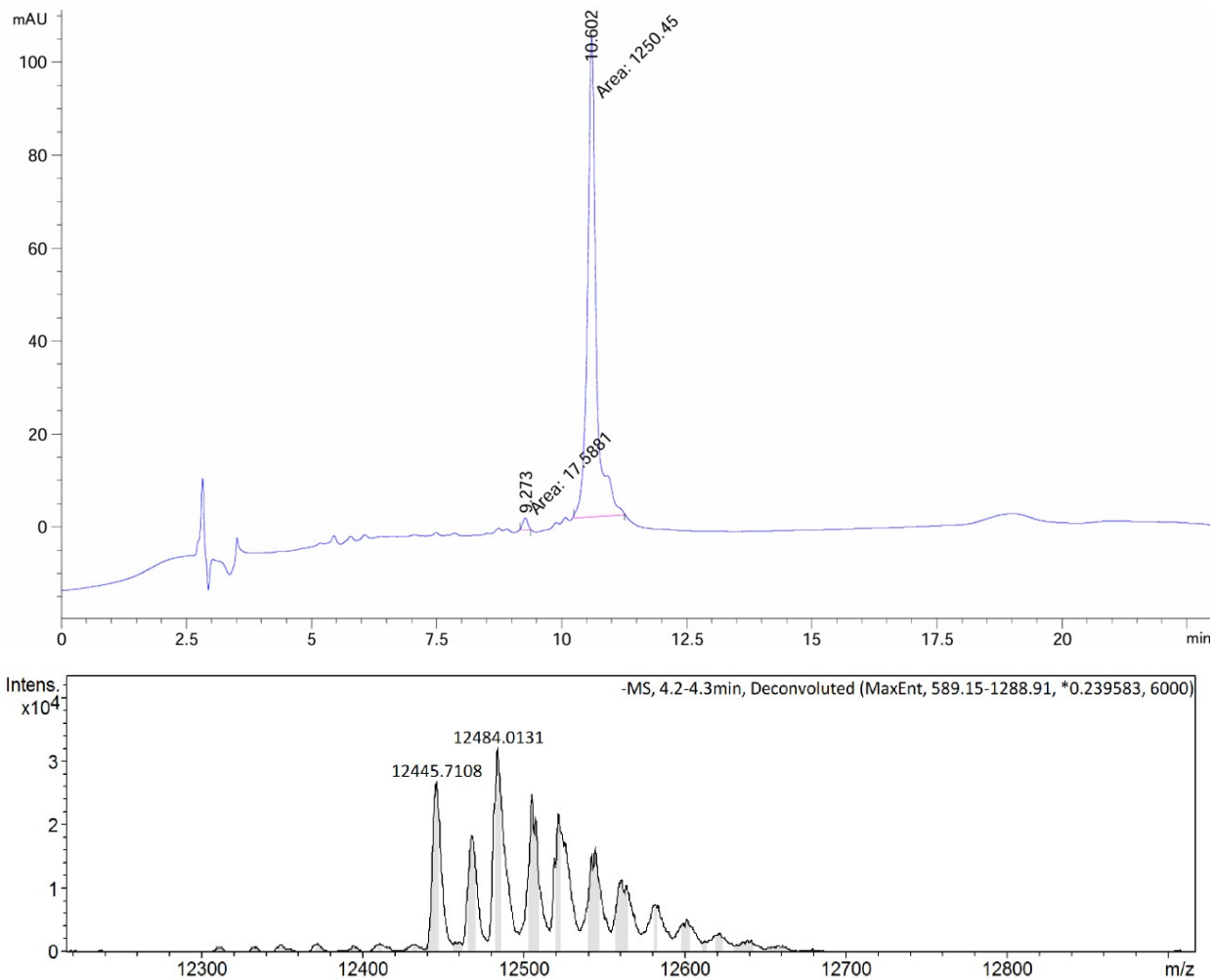


**Figure S1.** RP IP HPLC chromatogram and deconvoluted mass spectrum of the purified VA75A78 RNA template. RNA template [0.67 nM] analysis in H<sub>2</sub>O.

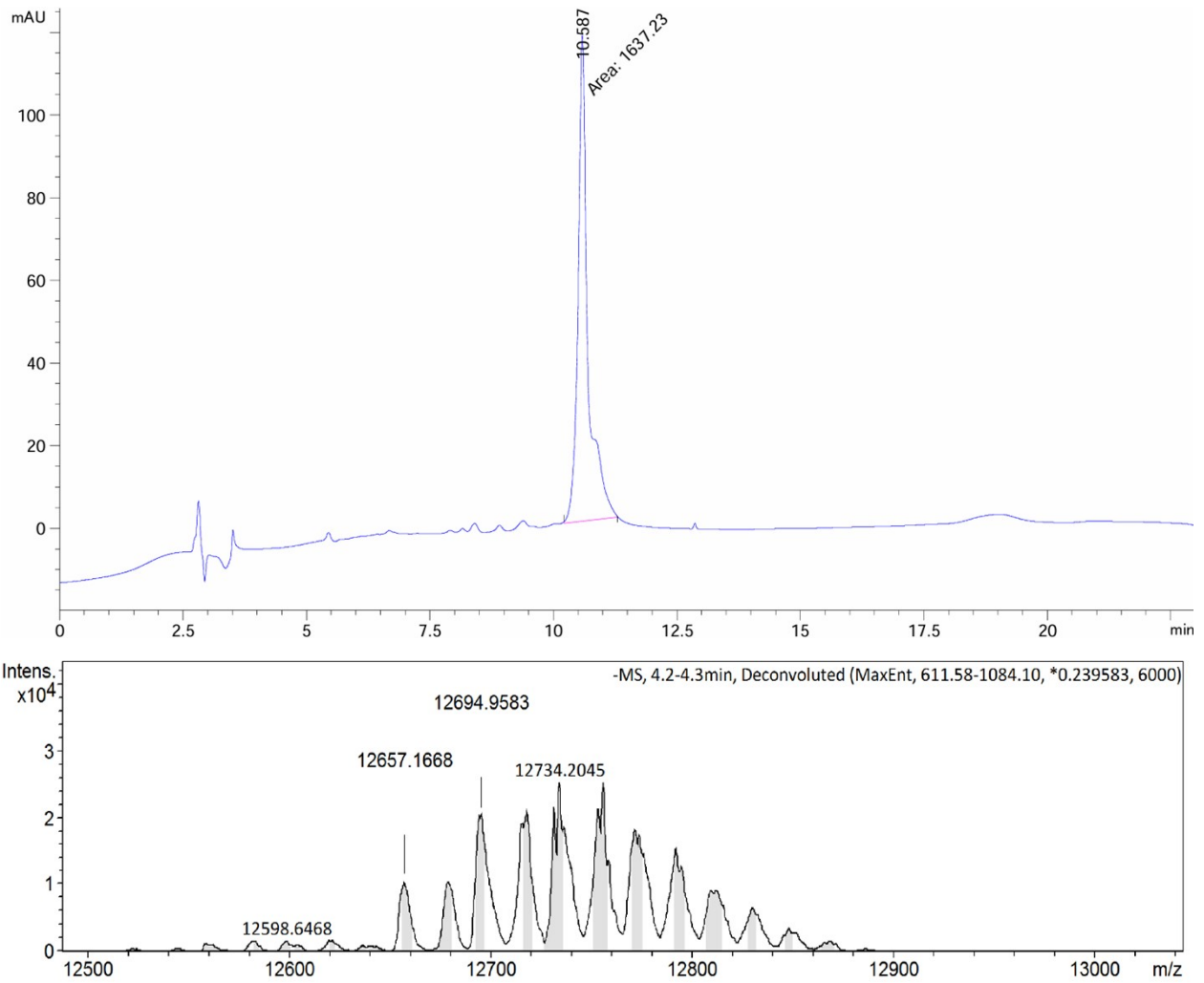


**Figure S2.** RP IP HPLC chromatogram and deconvoluted mass spectrum of purified VS75A170 RNA template. RNA template [0.67 nM] analysis in H<sub>2</sub>O.

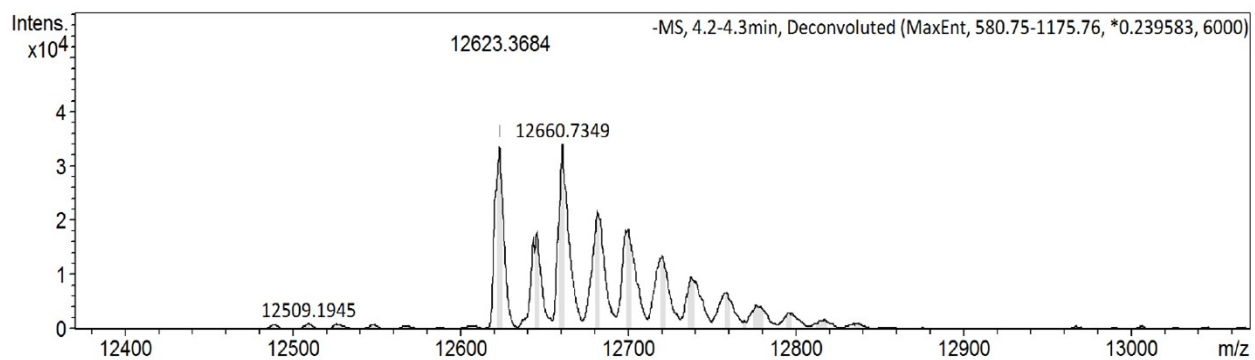
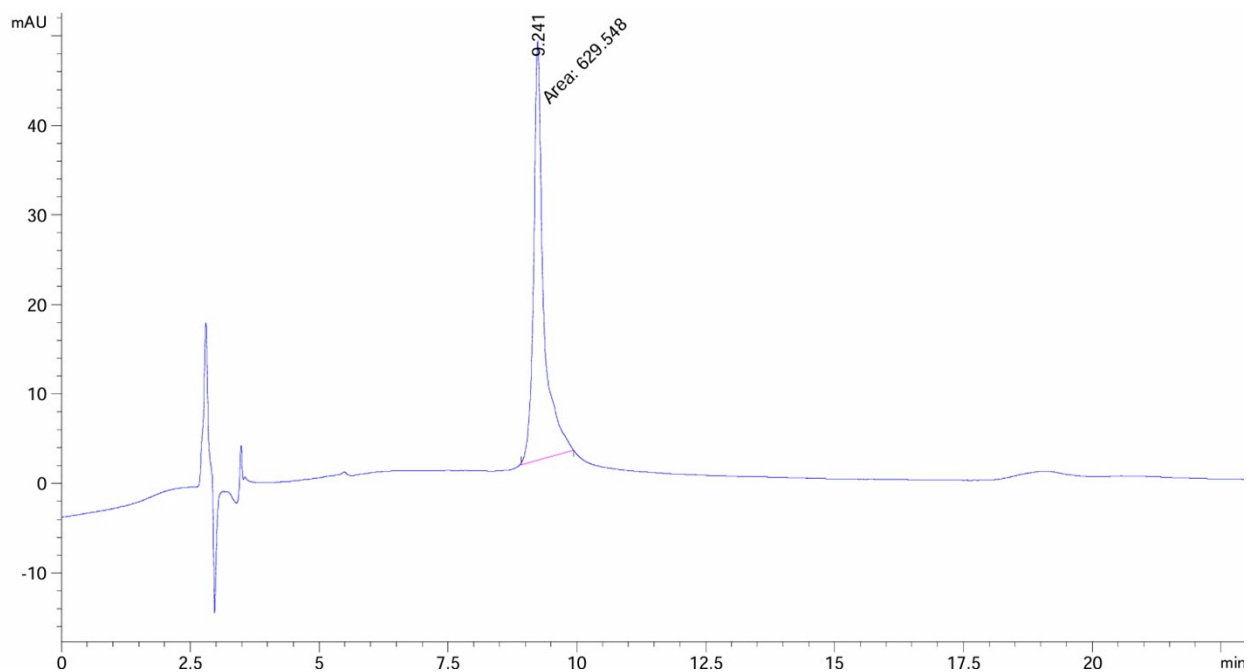


**Figure S3.** RP IP HPLC chromatogram and deconvoluted mass spectrum of purified VA94S78 RNA template. RNA template [0.67 nM] analysis in H<sub>2</sub>O.

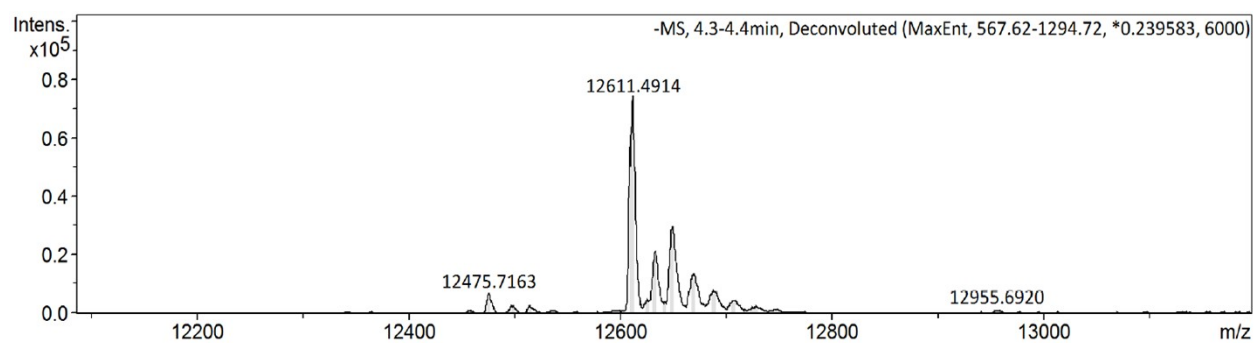
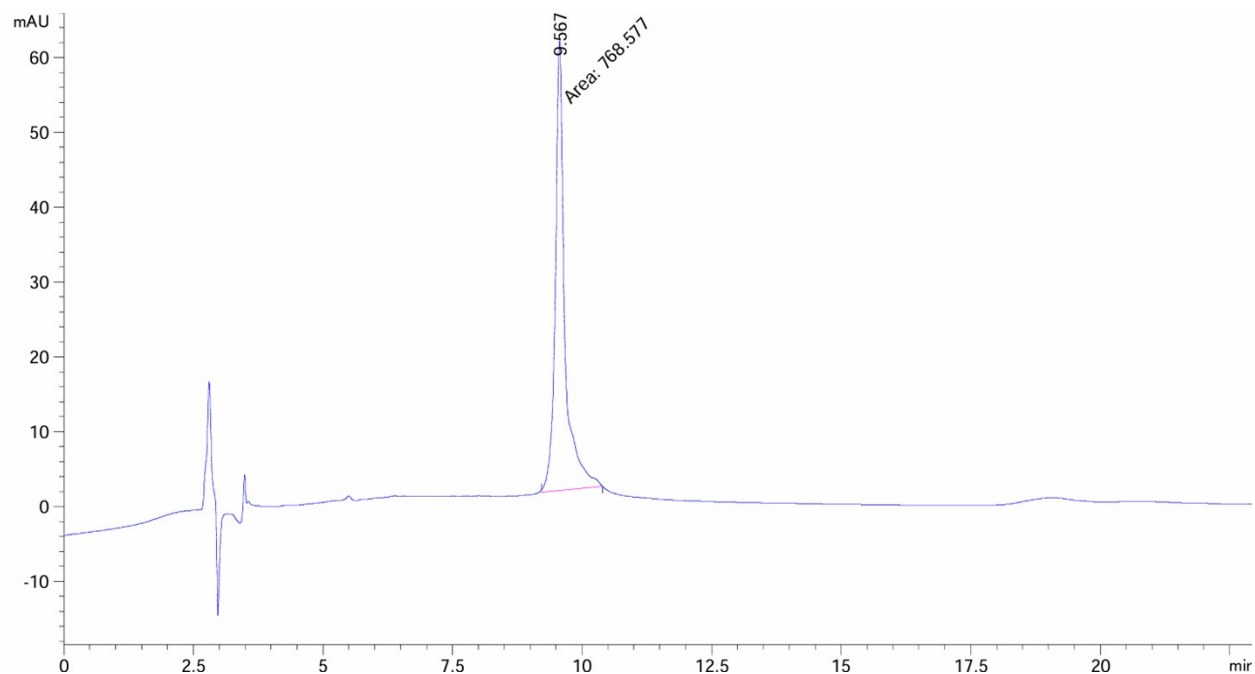


**Figure S4.** RP IP HPLC chromatogram and deconvoluted mass spectrum of purified VS94S170 RNA template. RNA template [0.67 nM] analysis in H<sub>2</sub>O.

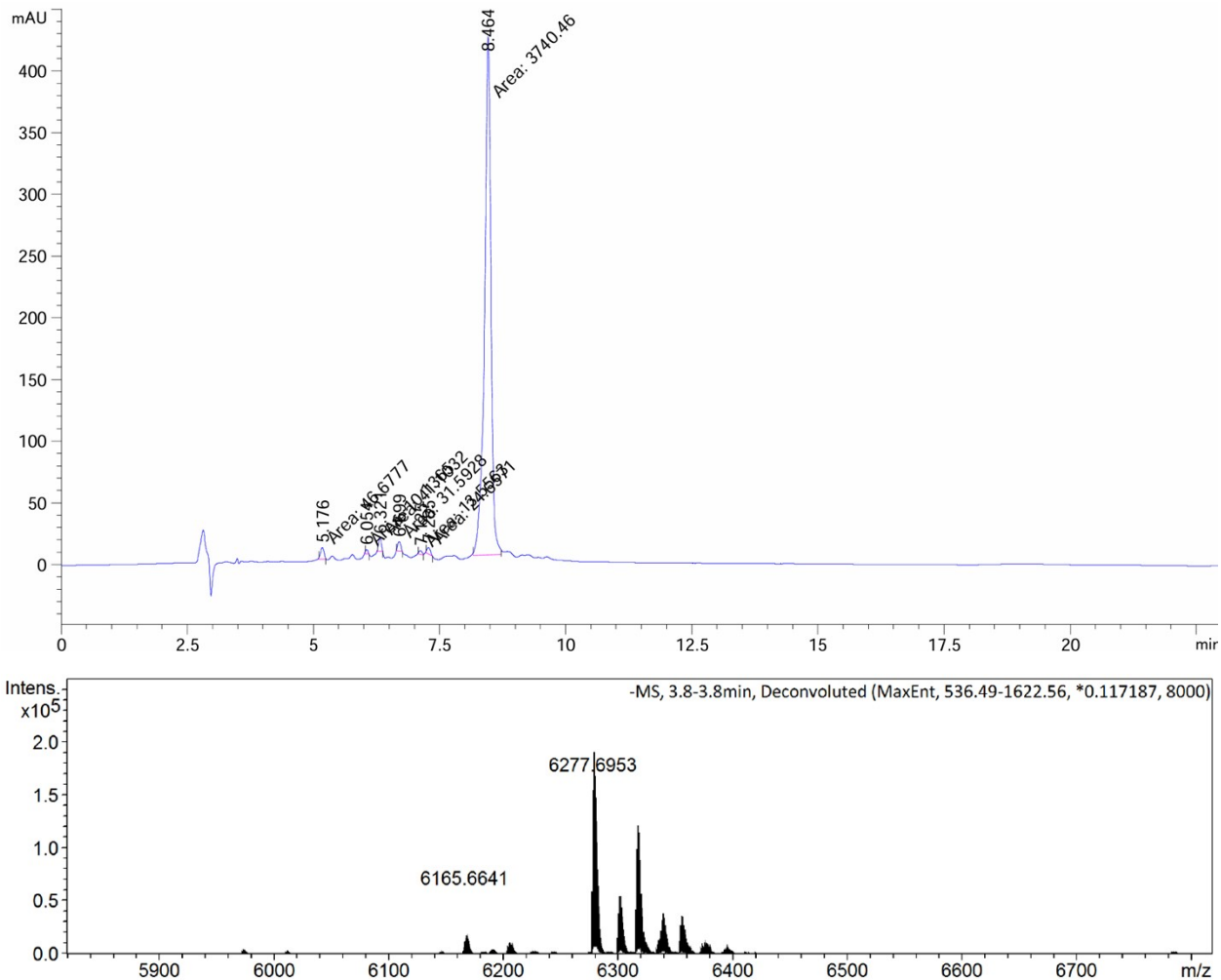


**Figure S5.** RP IP HPLC chromatogram and deconvoluted mass spectrum of purified 20-mer (A75) RNA control. RNA [1 nM] analysis in H<sub>2</sub>O.



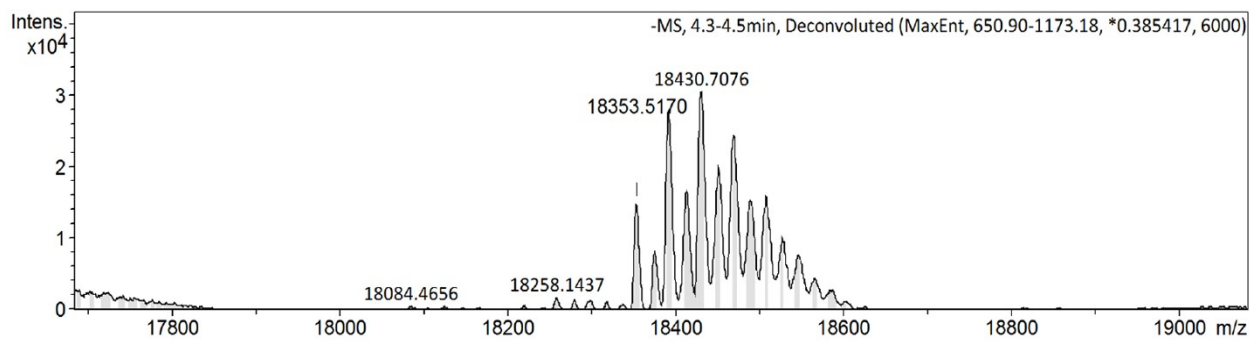
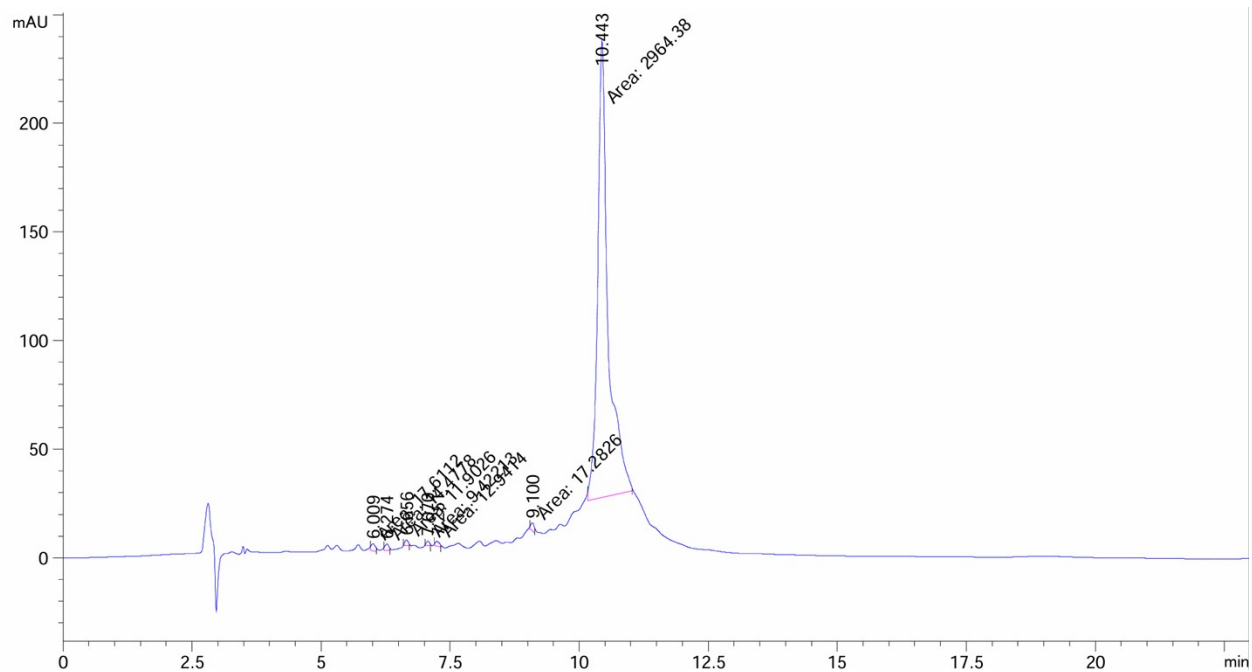


**Figure S7.** RP IP HPLC chromatogram and deconvoluted mass spectrum of purified 58-mer (A75A78A94) RNA control. RNA [1 nM] analysis in H<sub>2</sub>O.

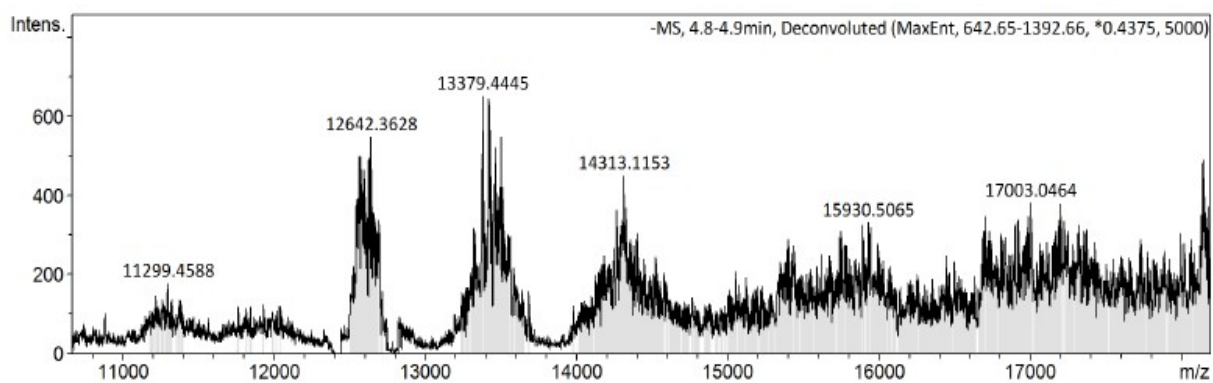
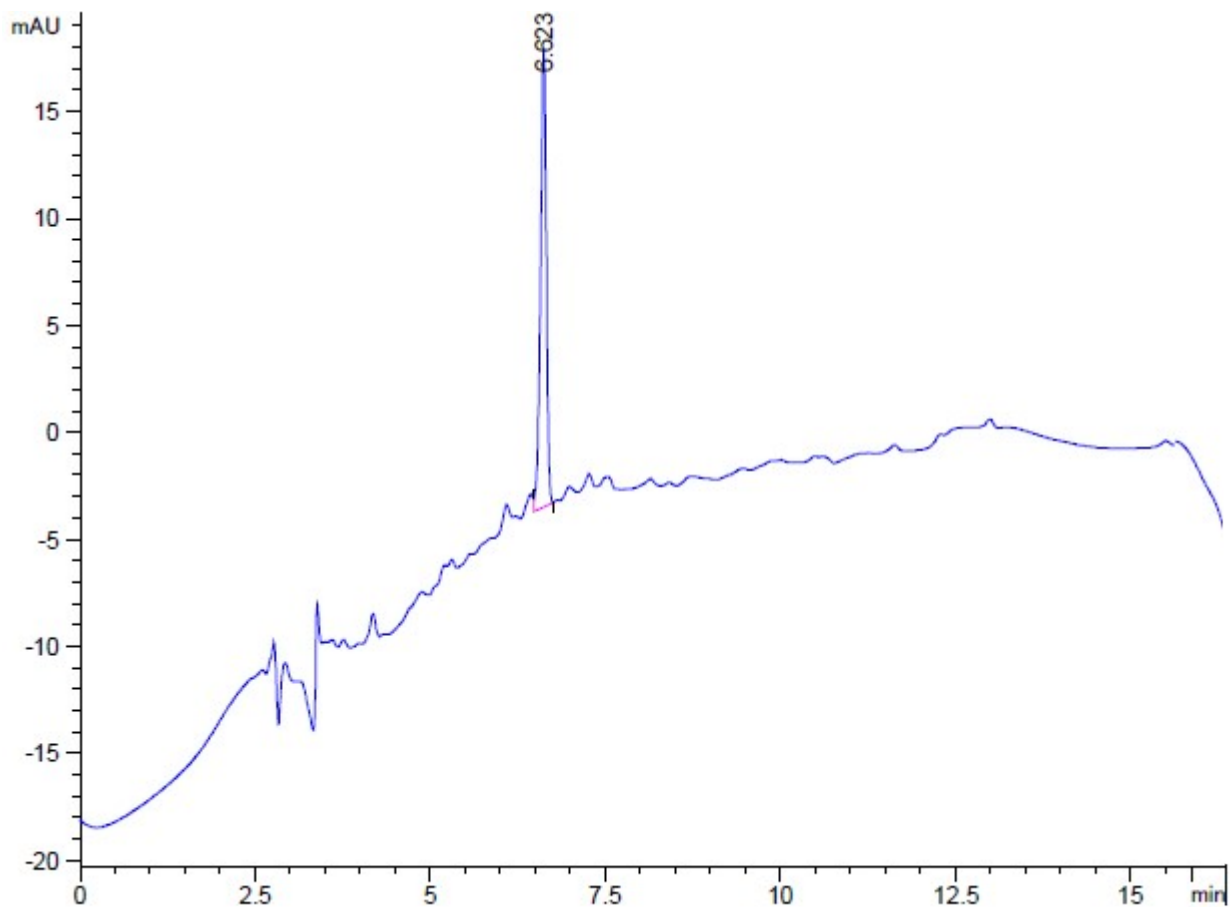


**Figure S8.** RP IP HPLC chromatogram of CM-labelled VS75A170 RNA template and deconvoluted mass spectrum of CM – VS75A170 RNA template. RNA [0.67 nM] analysis in H<sub>2</sub>O.

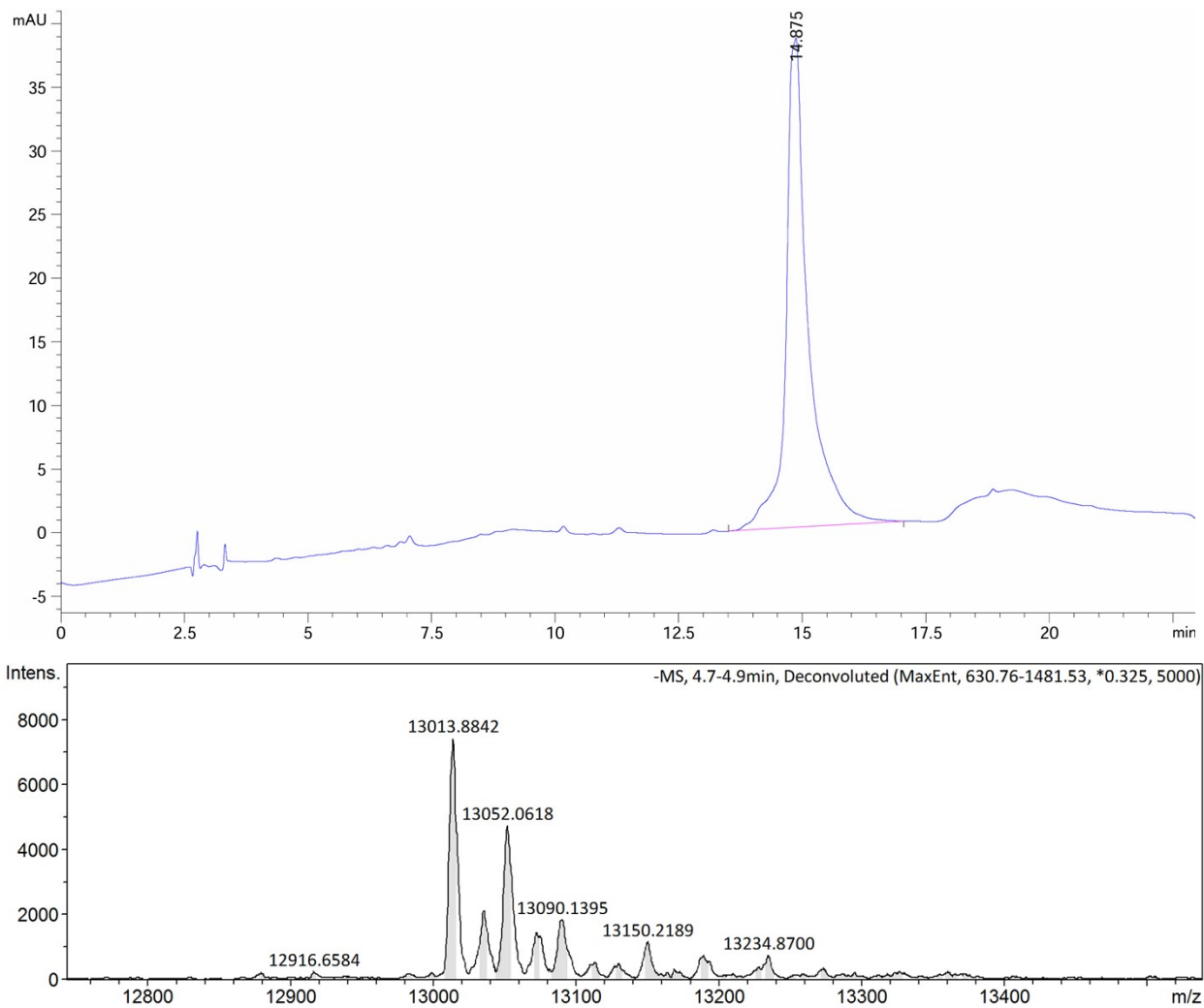


**Figure S9.** RP IP HPLC chromatogram and deconvoluted mass spectrum of pure FITC-labelled VA75A78 RNA template. RNA [0.67 nM] analysis in H<sub>2</sub>O.

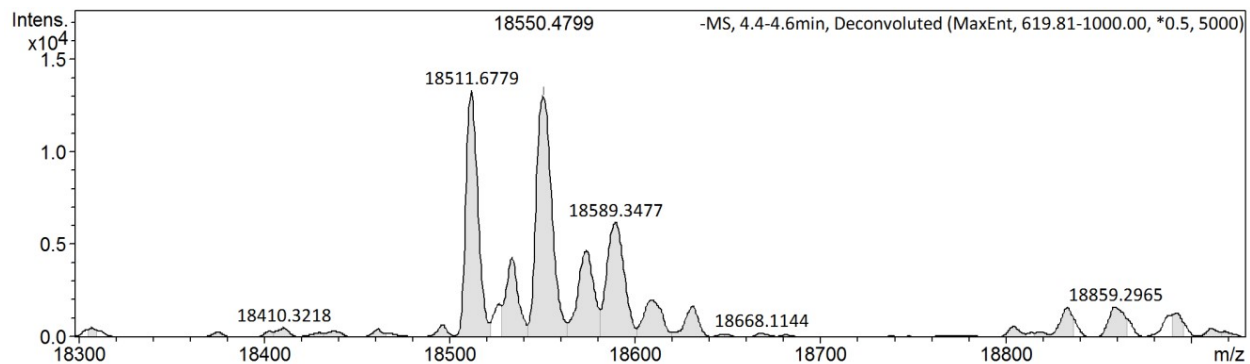
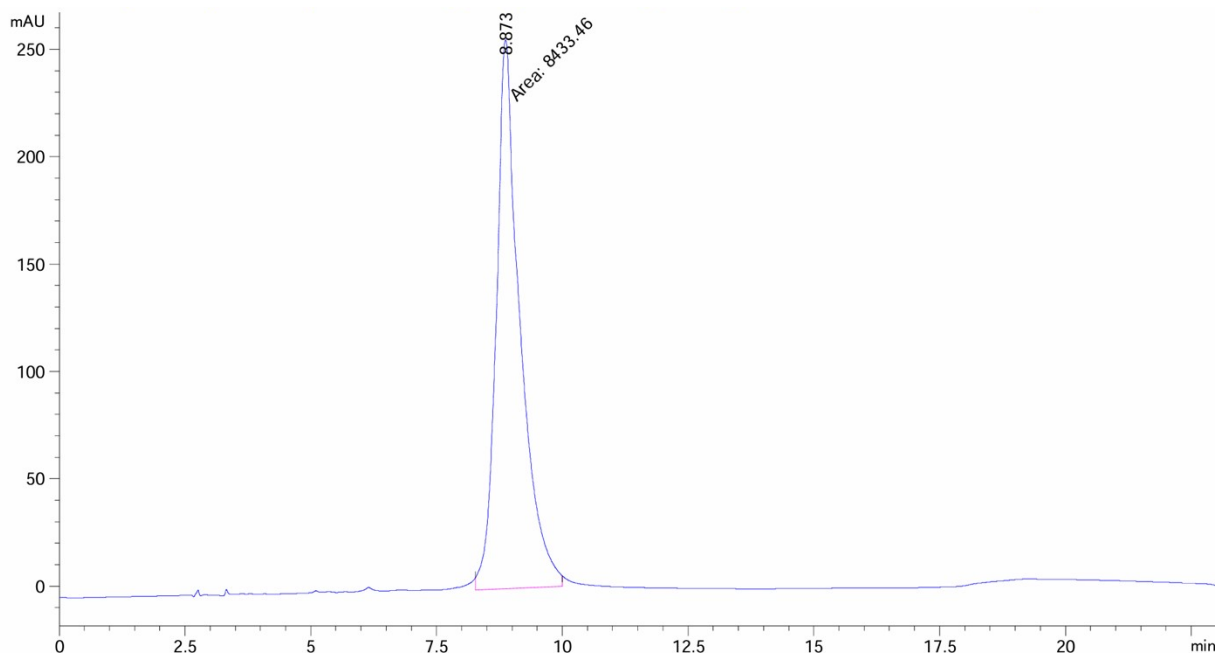


**Figure S10.** RP IP HPLC chromatogram and deconvoluted mass spectrum of purified Cube 1 Y-template. RNA [0.33 nM] analysis in H<sub>2</sub>O.

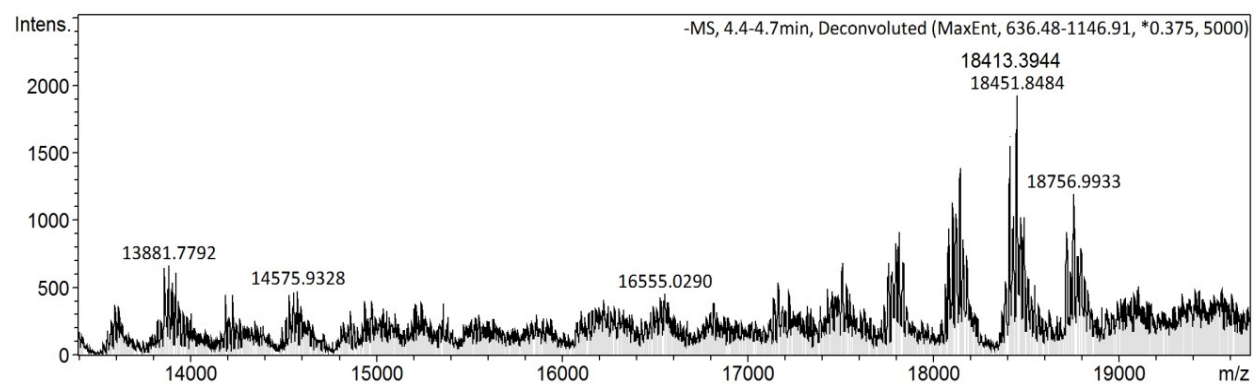
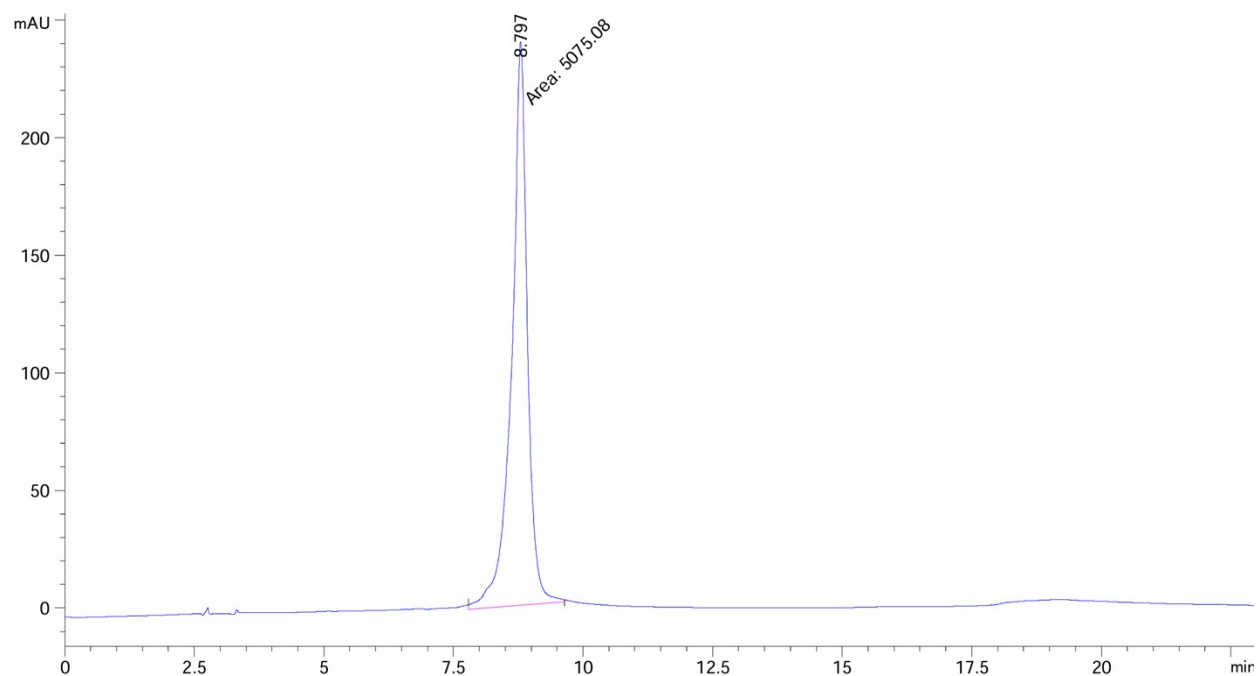


**Figure S11.** RP IP HPLC chromatogram and deconvoluted mass spectrum of purified Cube 2 Y-template. RNA [0.33 nM] sample analysis in H<sub>2</sub>O.

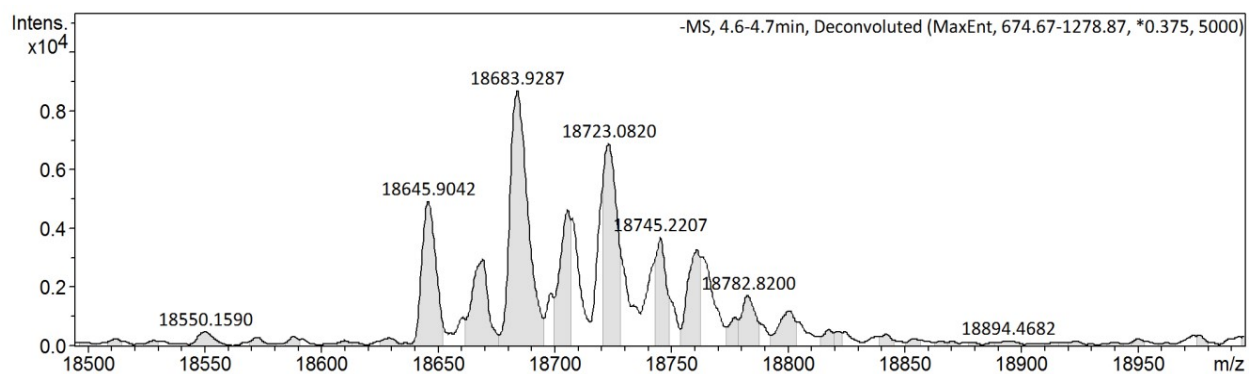
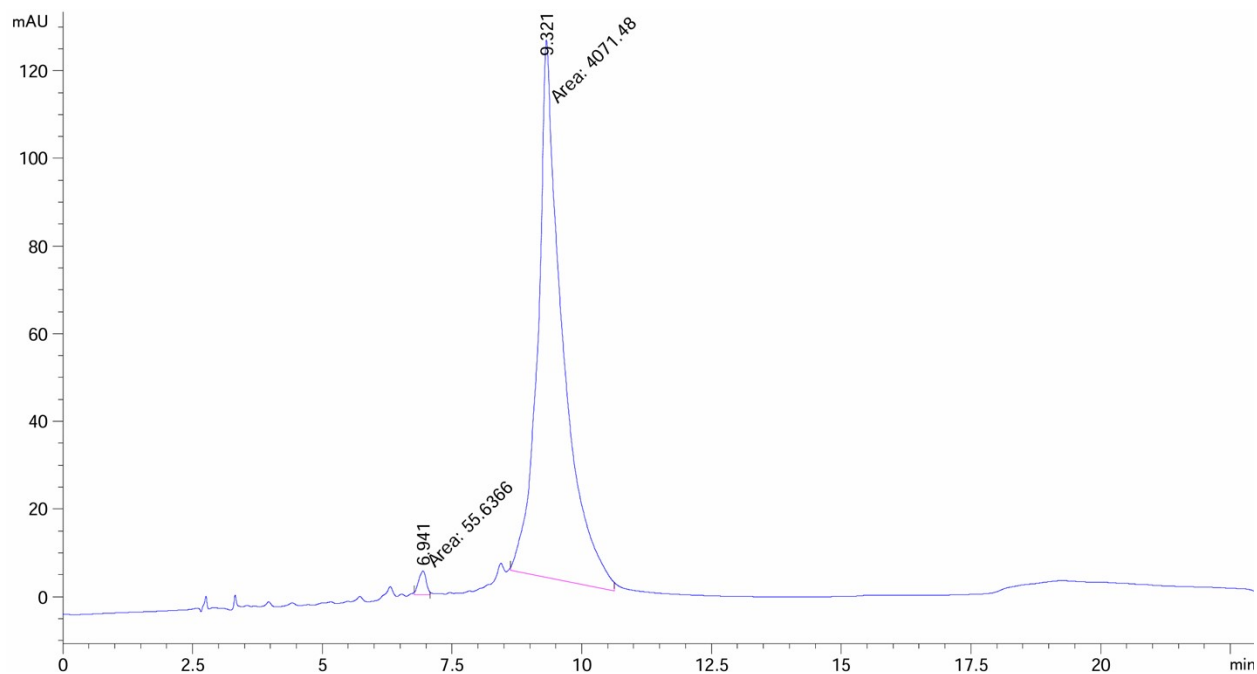


**Figure S12.** RP IP HPLC chromatogram and deconvoluted mass spectrum of purified Cube 3 Y-template. RNA [0.33 nM] analysis in H<sub>2</sub>O.

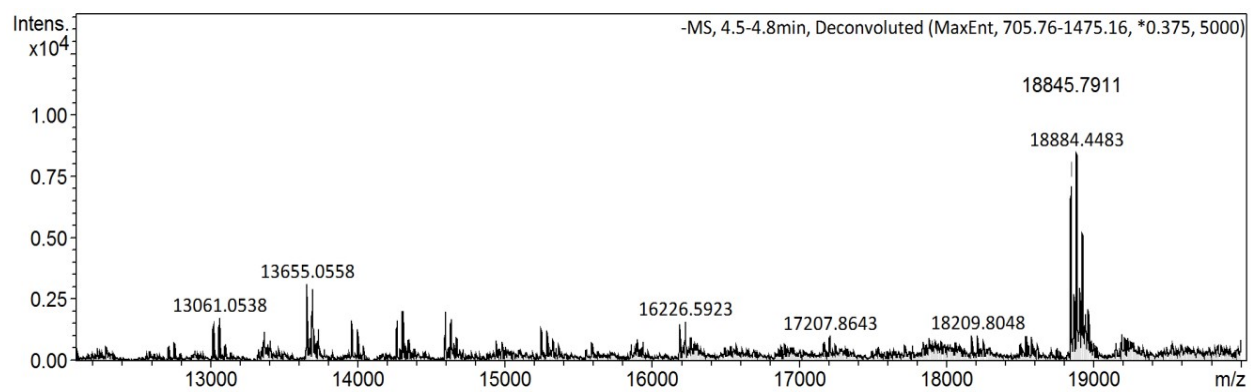
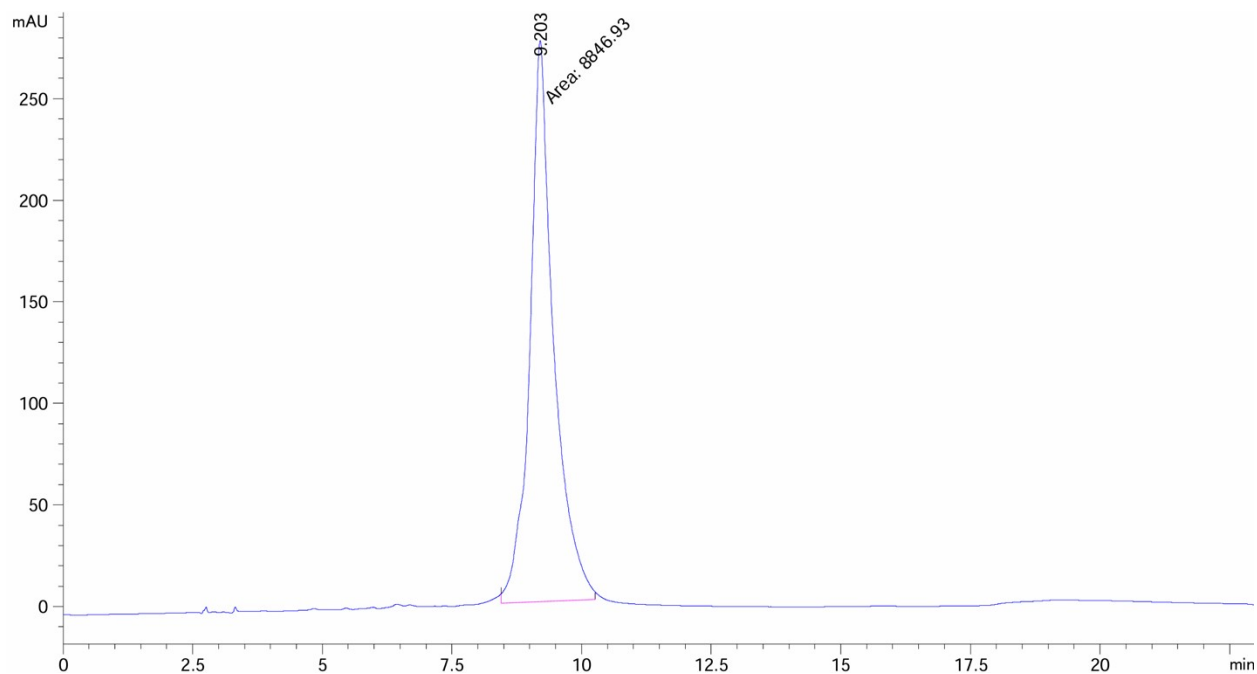


**Figure S13.** RP IP HPLC chromatogram and deconvoluted mass spectrum of purified Cube 4 Y-template. RNA [0.33 nM] analysis in H<sub>2</sub>O.

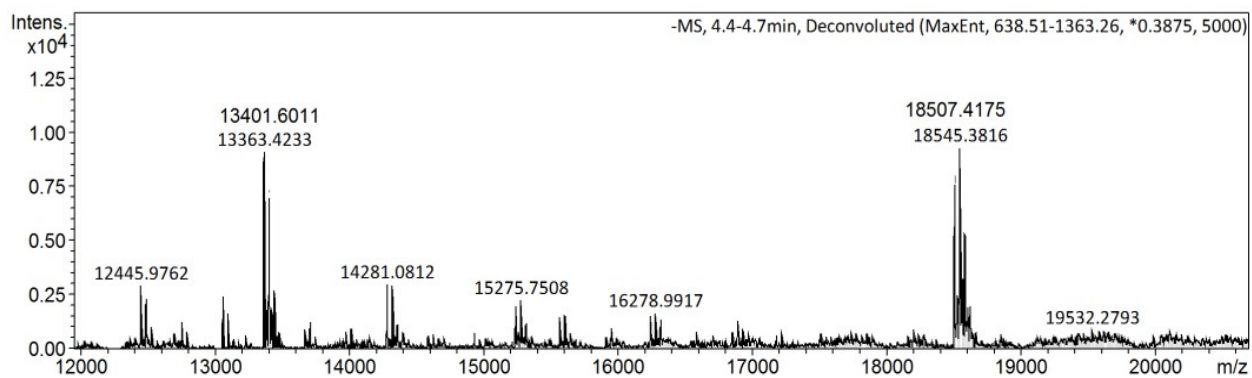
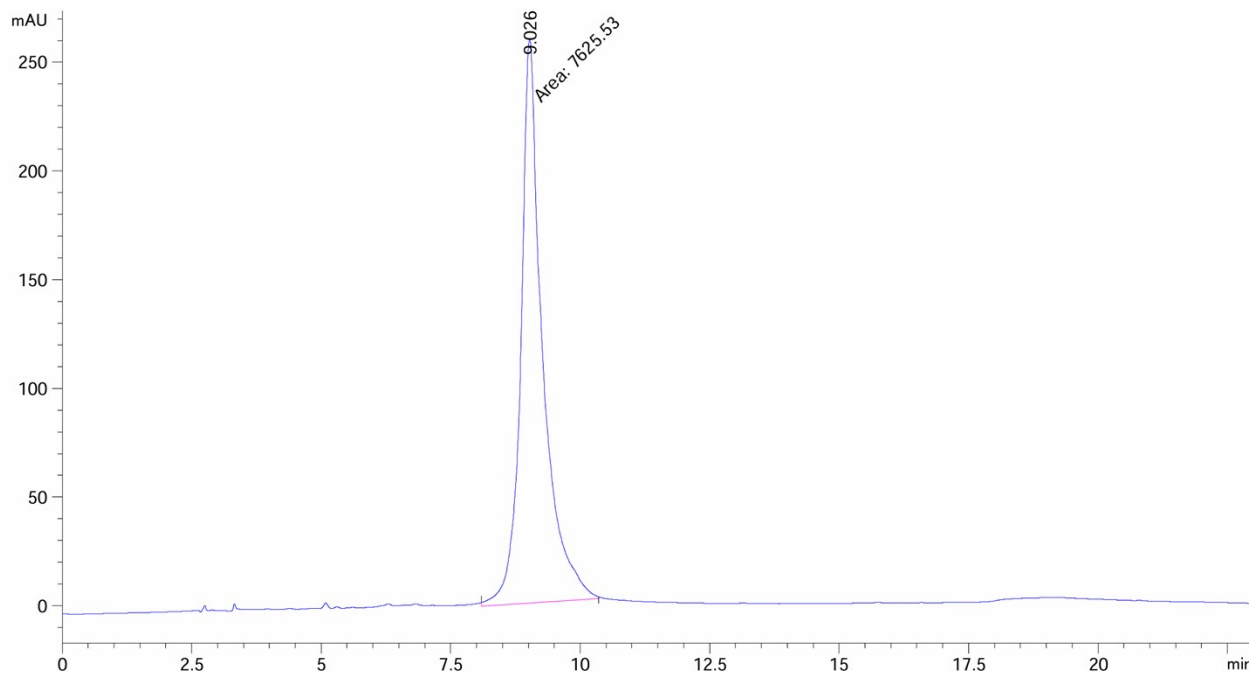


**Figure S14.** RP IP HPLC chromatogram and deconvoluted mass spectrum of purified Tube 1 Y-template. RNA [0.33 nM] analysis in H<sub>2</sub>O.

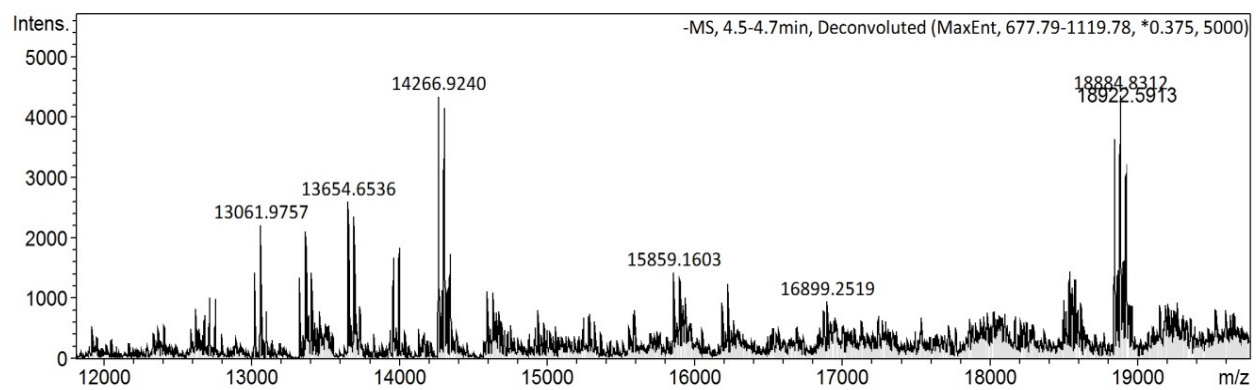
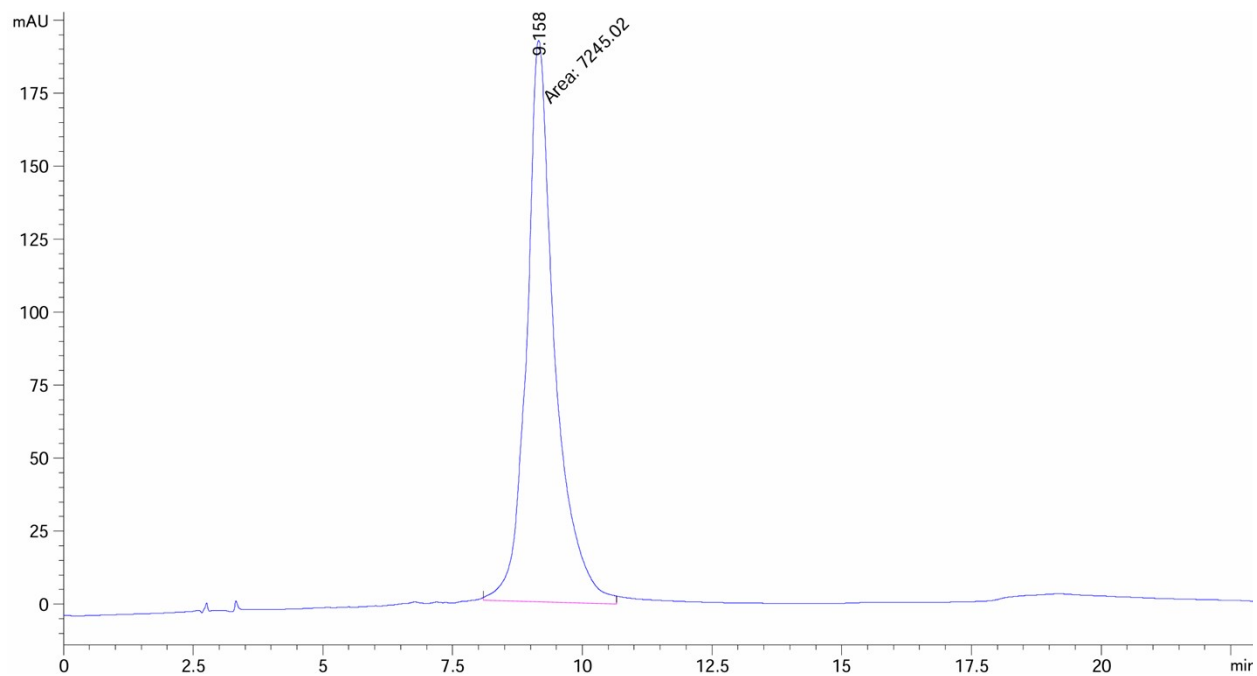


**Figure S15.** RP IP HPLC chromatogram and deconvoluted mass spectrum of purified Tube 2 Y-template. RNA analysis [0.33 nM] in H<sub>2</sub>O.

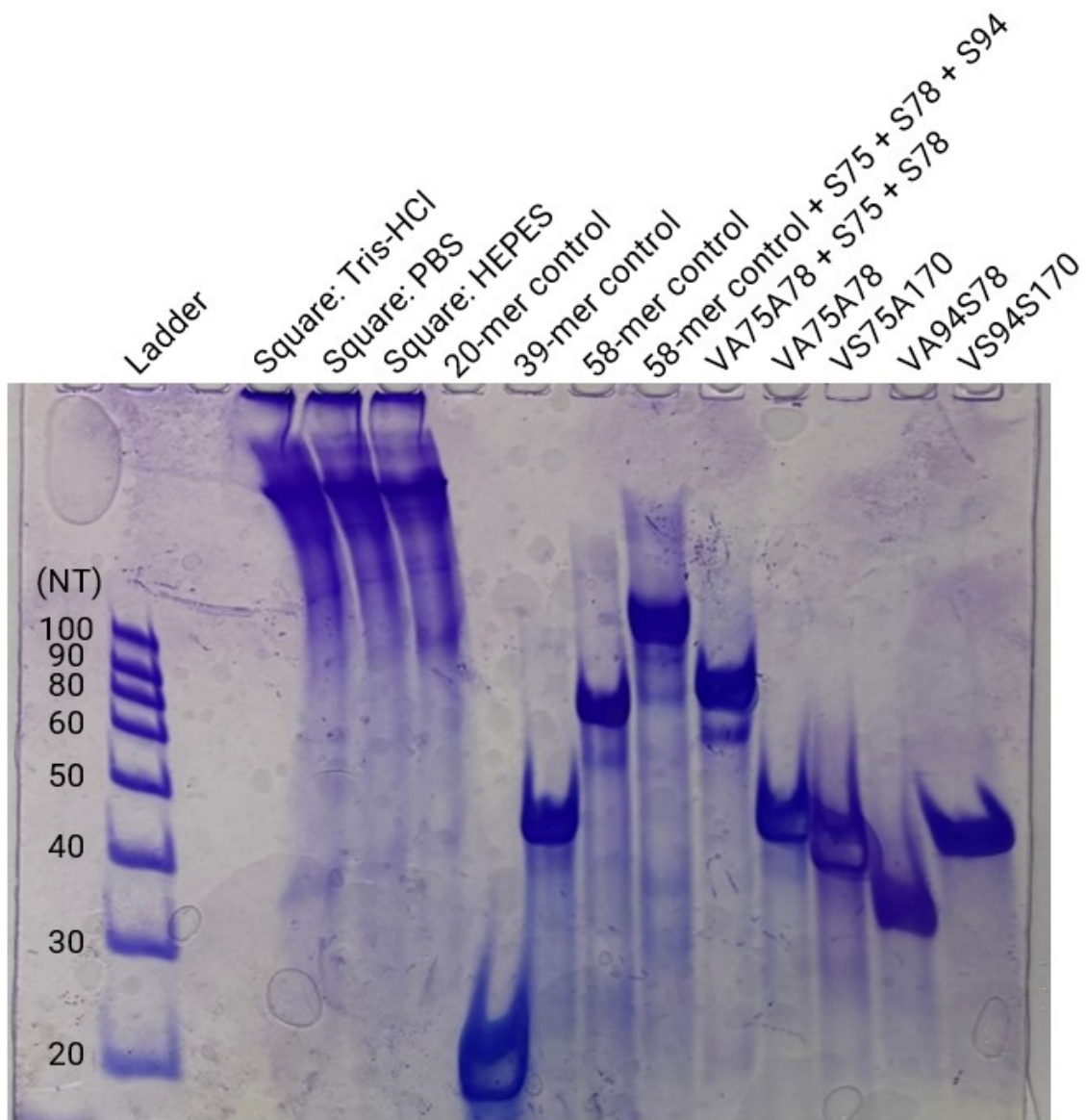
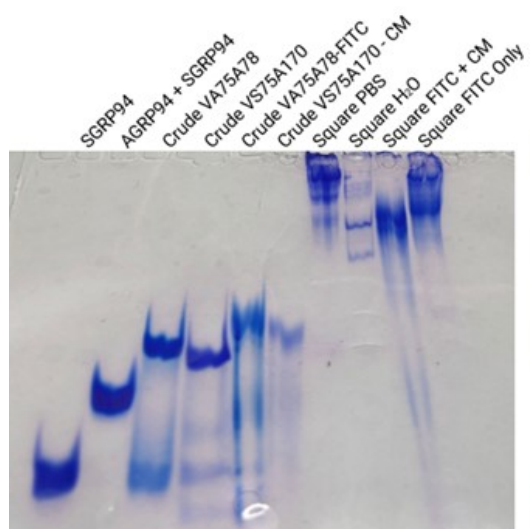
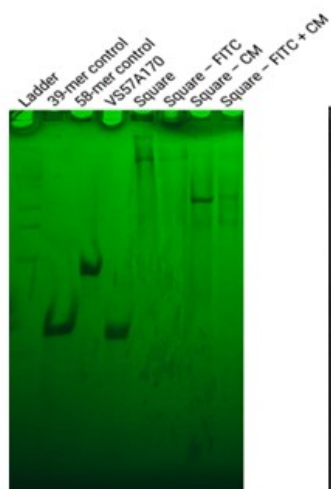


**Figure S16.** Native (20%) PAGE of hybrid V-shape RNA templates for square-shape assembly. Gel image visualized by Stains-All™.

A.



B.



C.

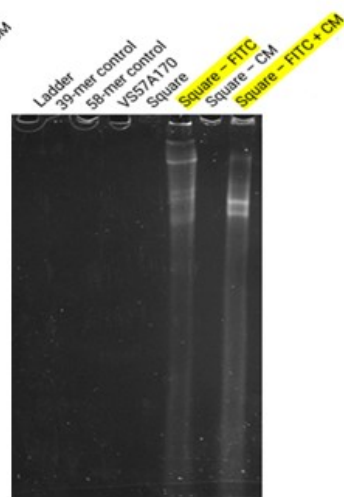


**Figure S17.** Native (20%) PAGE of hybrid fluorescently labelled FITC and CM-labelled RNA V-templates for square shape assembly. Gel images also compare the hybrid assembly stability in buffer (PBS) and H<sub>2</sub>O. Gel images visualized by (A) Stains-All, and under (B) low-UV at 254 nm and (C) high-UV at 450 nm shadowing, displaying FITC fluorescence in highlighted samples.

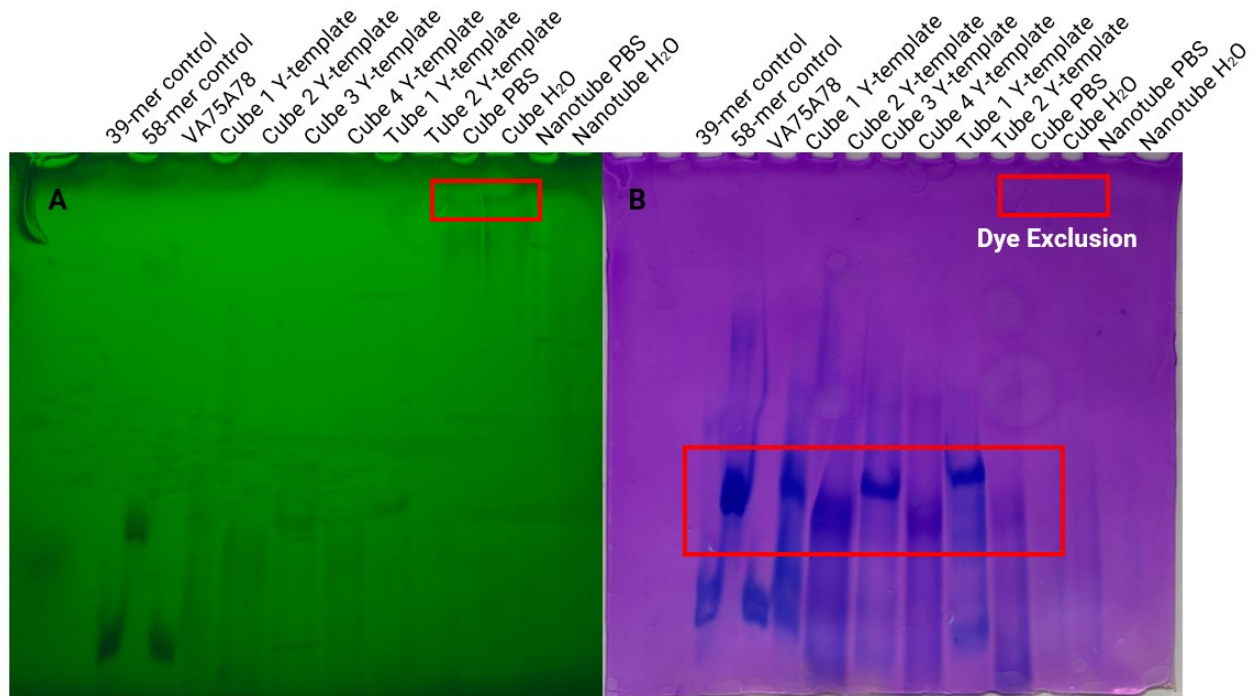


**Figure S18.** Native (14%) PAGE of RNA Y-shape templates for the assembly of the putative cube and tube structures with gel imaging under UV-shadowing at 254 nm (A) and (B) Stains-All.

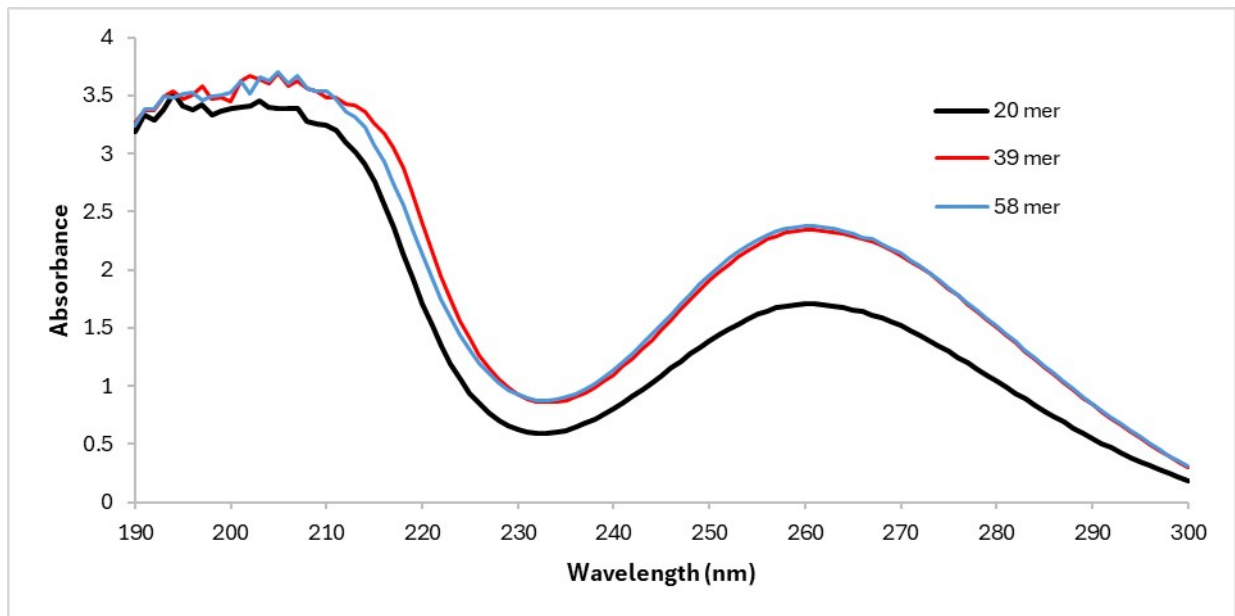


**Figure S19.** Ultraviolet visible (UV-Vis) absorption spectra of 20-mer (A75), 39-mer (A75A78), and 58-mer (A75A78A94) single stranded RNA controls. All samples were prepared in H<sub>2</sub>O.

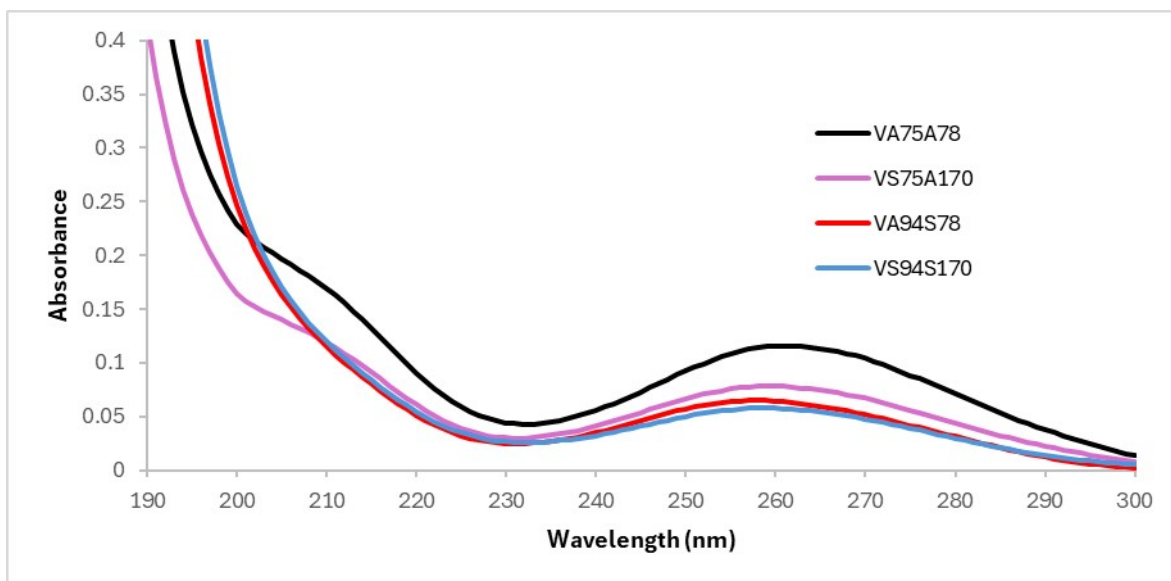


**Figure S20.** Ultraviolet visible (UV-Vis) absorption spectra of purified V-shape RNA templates, VA75A78, VS75A170, VA94S78, and VS94S170. All samples were prepared in H<sub>2</sub>O.

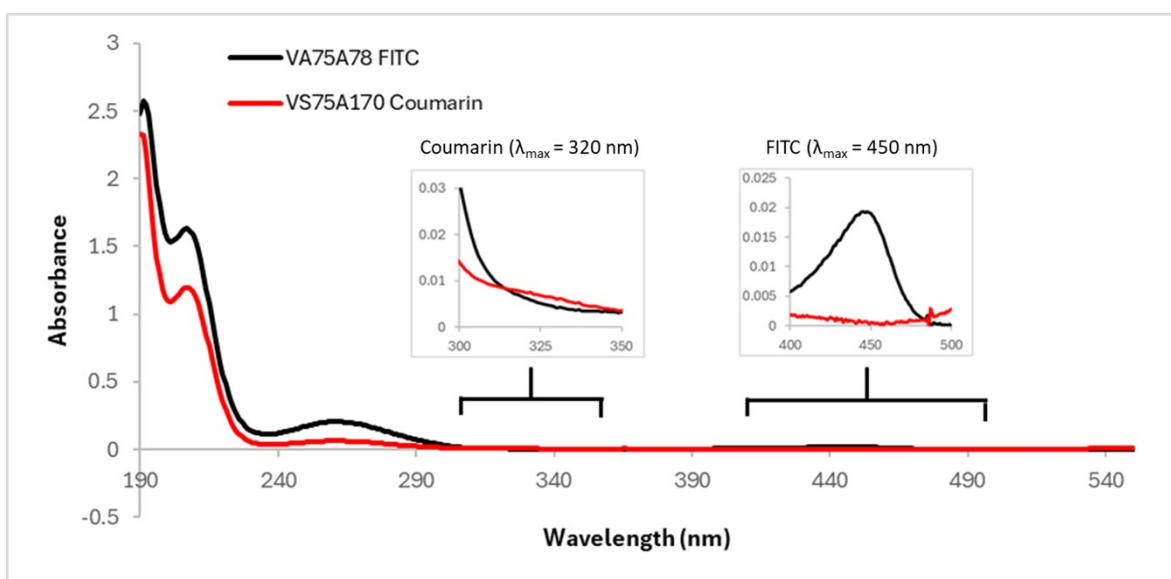


**Figure S21.** Ultraviolet visible (UV-Vis) absorption spectra of purified fluorochrome (FITC and CM) labelled V-shape RNA templates, FITC-VA75A78 and CM-VS75A170. Insets demonstrate CM ( $\lambda_{\text{max}} = 320 \text{ nm}$ ) and FITC ( $\lambda_{\text{max}} = 450 \text{ nm}$ ) absorbance bands. All samples were prepared in H<sub>2</sub>O.

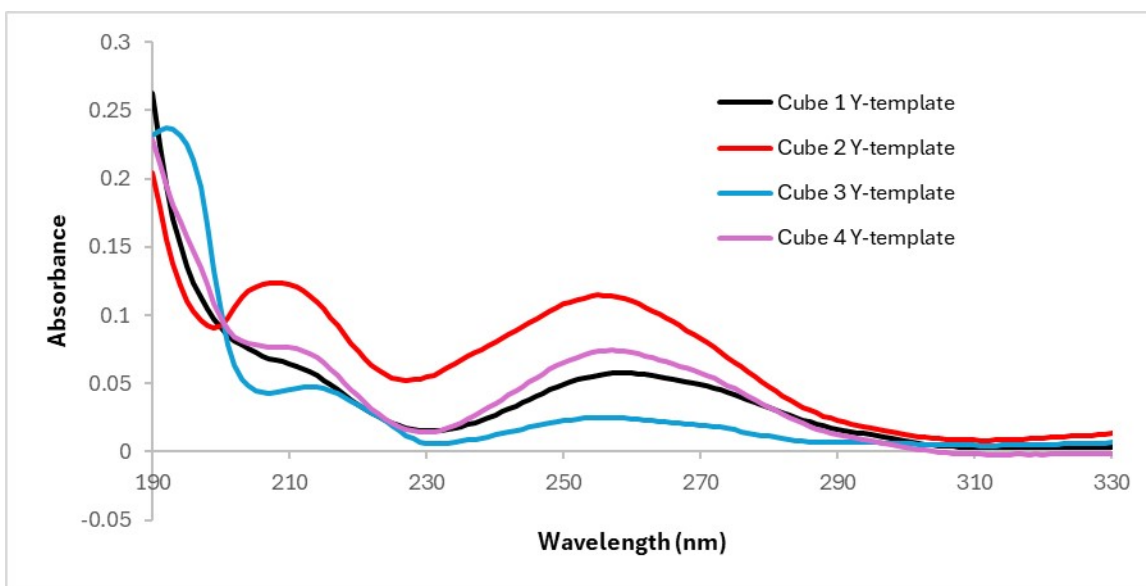


**Figure S22.** Ultraviolet visible (UV-Vis) absorption spectra of purified Y-shape RNA templates for Cube 1, Cube 2, Cube 3, and Cube 4. All samples were prepared in H<sub>2</sub>O.

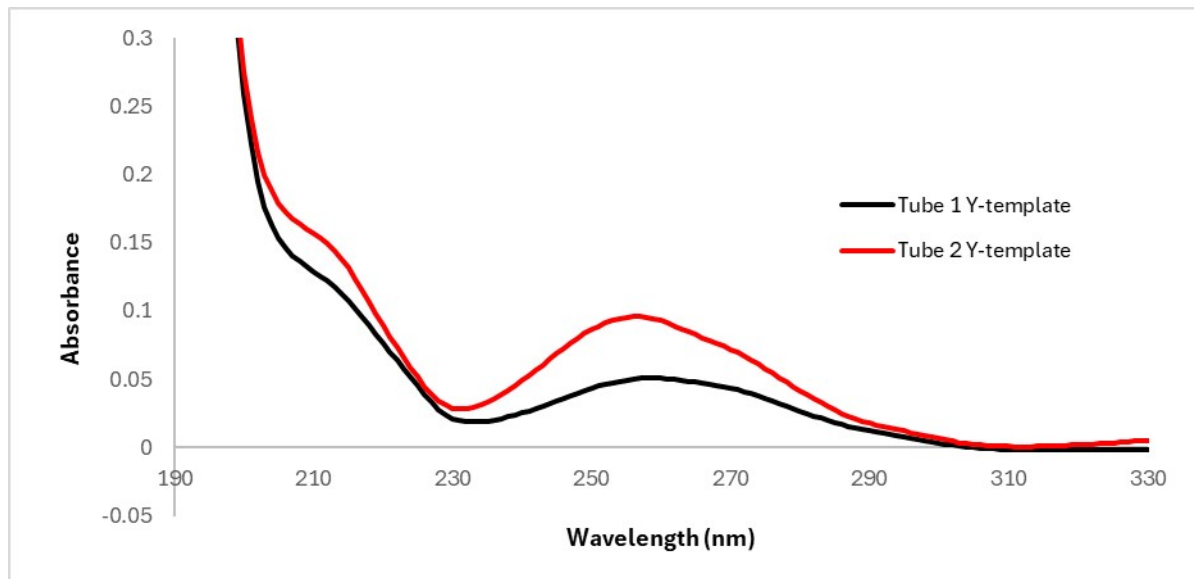


**Figure S23.** Ultraviolet visible (UV-Vis) absorption spectra of purified Y-shape RNA templates for Tube 1 and Tube 2. All samples were prepared in H<sub>2</sub>O.

A.

B.

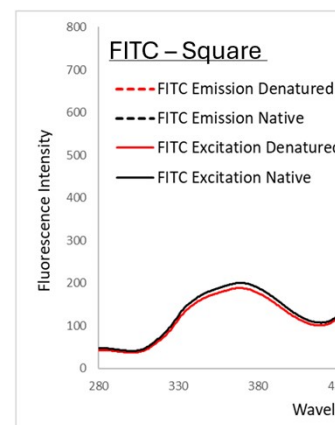


**Figure S24.** Fluorescence excitation and emission spectra collected under native (hybrid assembly) and denatured (ssRNA) forms for the (A) FITC – Square RNA and (B) CM – Square assembly. (FITC:  $\lambda_{\text{ex}} = 492 \text{ nm}$ ,  $\lambda_{\text{em}} = 520 \text{ nm}$ . CM:  $\lambda_{\text{ex}} = 320 \text{ nm}$ ,  $\lambda_{\text{em}} = 420 \text{ nm}$ ).

A.

B.

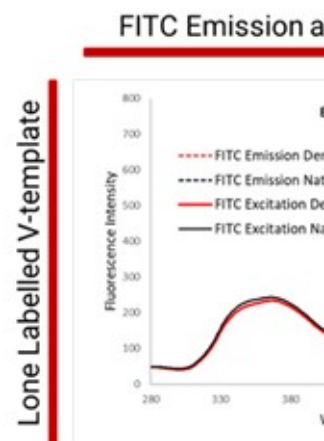


**Figure S25.** FRET analysis of (A) FITC- and (B) CM-labelled RNA V-shape templates alone, under native and denatured conditions.

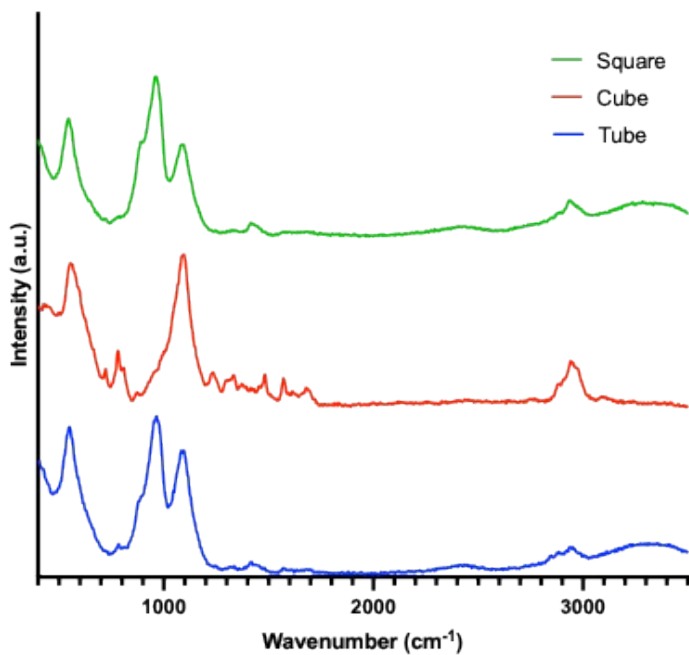


**Figure S26.** Raman spectra of the RNA nanostructures (1  $\mu$ M, square, cube, and tube) in H<sub>2</sub>O.

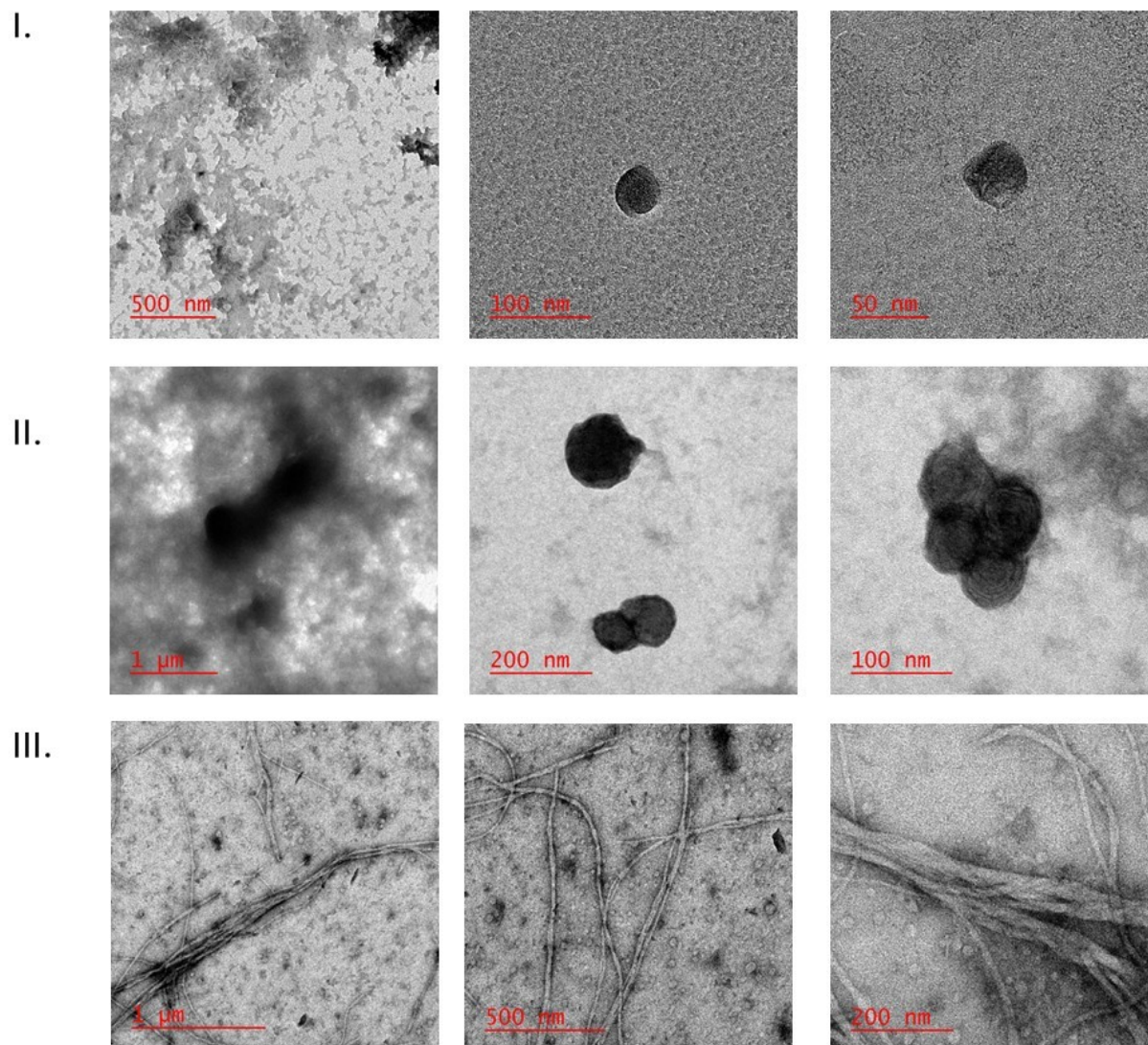


**Figure S27.** Supplemental TEM images at various scale (50 nm – 1 μm) magnifications showing closer and broad-field views of the RNA nanostructures (1 μM in H<sub>2</sub>O) representing I. squares, II. cubes and III. tubes.

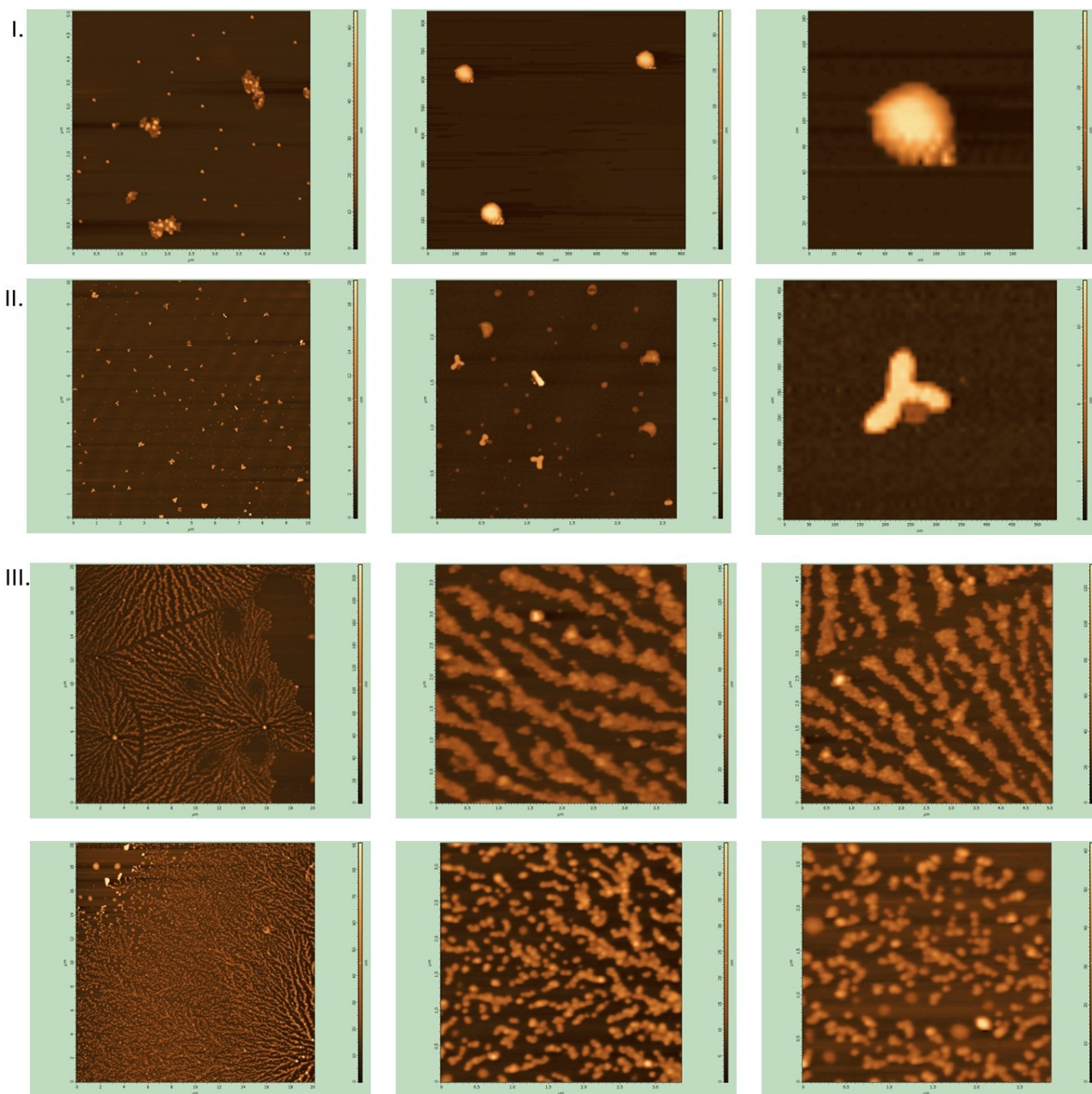


**Figure S28.** AFM images of the (I) square, (II) cube and (III) tube RNA nanostructures (0.1-1  $\mu\text{M}$  in  $\text{H}_2\text{O}$ ).

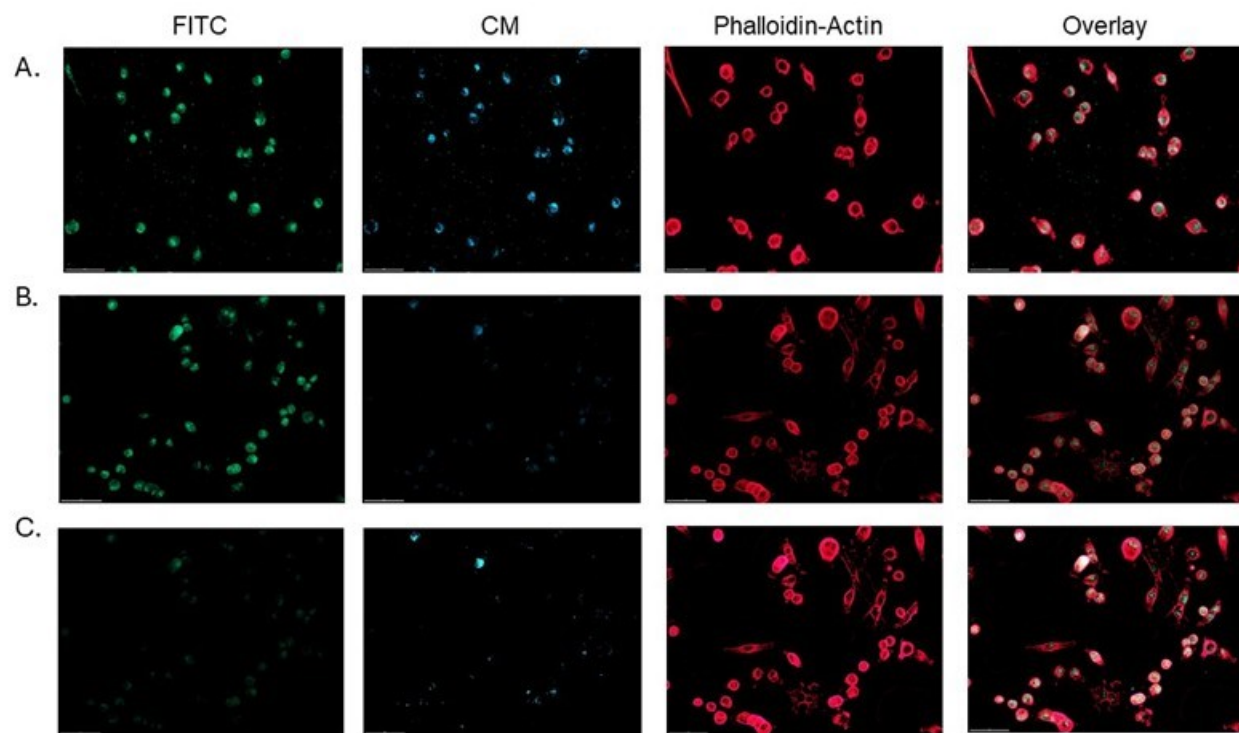


**Figure S29.** Fluorescence microscopy of (A) FITC+CM, (B) FITC, and (C) CM, labelled square-shape siRNA (50 nM) with Lipofectamine-based transfection in EMEM and 10% FBS in the A549 cells incubated for 4 h at 37 °C prior to fluorescence imaging. Scale bars set at 20 mm.

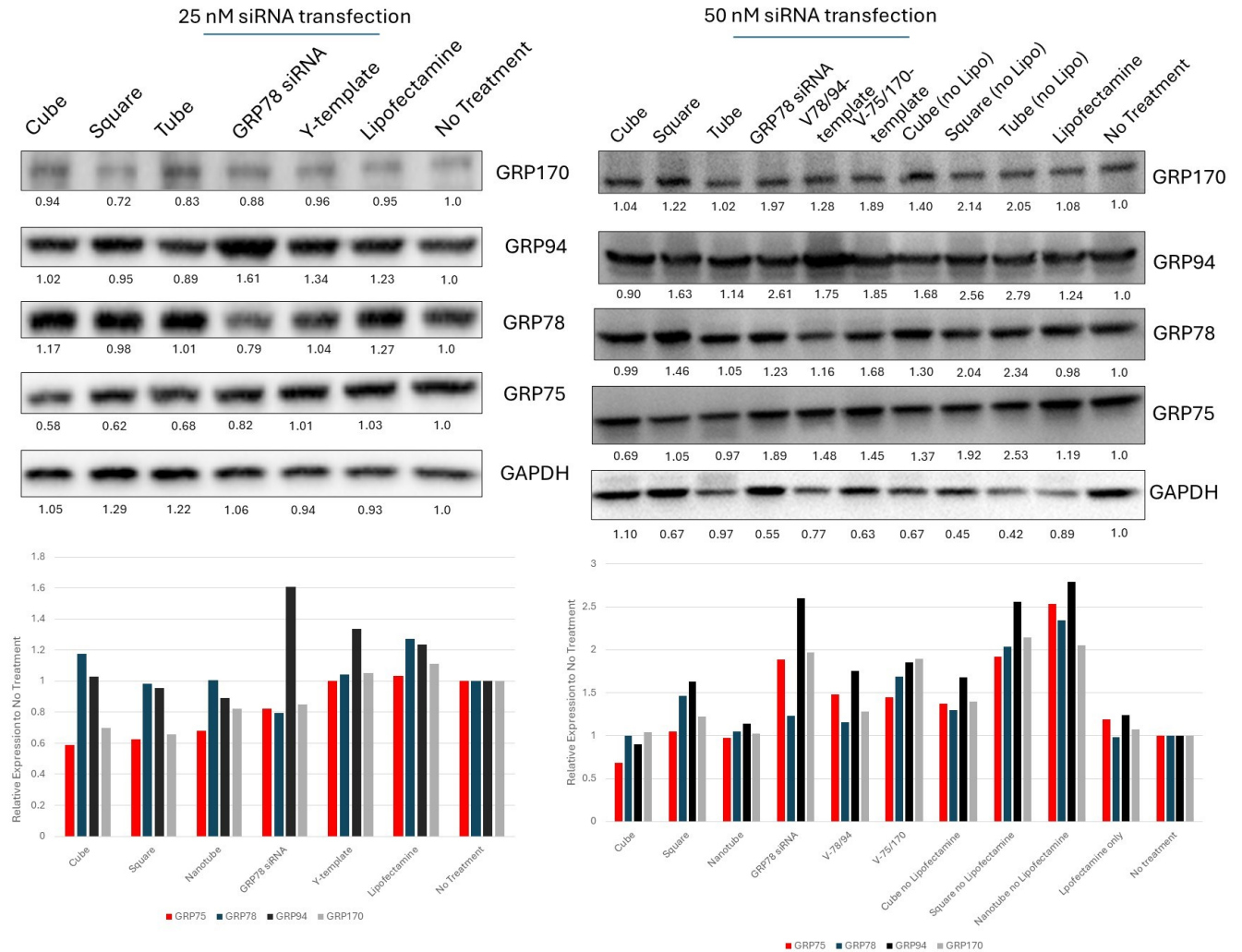


**Figure S30.** Comparative western blot data of GRP75, GRP78, GRP94 and GRP170, normalized and quantitated against the loading control, GAPDH, that was also normalized against the no treatment conditions, and analyzed using monoclonal primary antibodies and HRP-conjugated secondary antibody following dose-dependent (25 vs 50 nM) transfections of the siRNA nanostructures (cube, square and tube with and without Lipofectamine, Lipo) along with GRP78 siRNA, V-, Y-templates and vehicle controls with Lipofectamine 3000™ (4-6 μL) as transfection reagent in DMEM cell culture media supplemented with 10% FBS over a 66 h period in a humidified incubator set at 37 °C with 5% CO<sub>2</sub>.

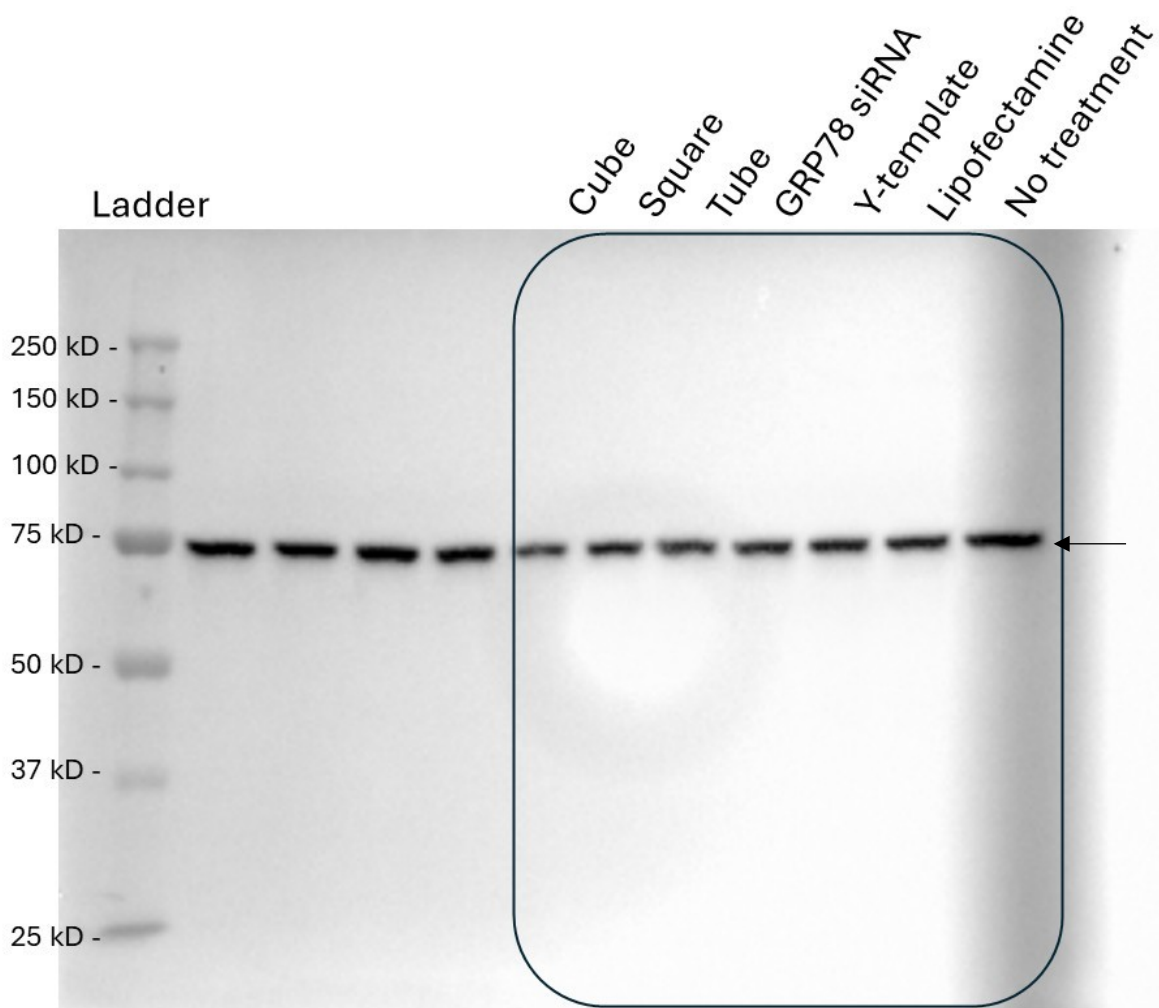


**Figure S31.** Full western blot image of GRP75 using primary monoclonal anti-GRP75 and HRP-conjugated secondary antibody following siRNA transfections (25 nM) of the siRNA nanostructures (cube, square and tube) along with GRP78 siRNA, Y-template and vehicle controls with Lipofectamine 3000™ (6  $\mu$ L) in DMEM cell culture media supplemented with 10% FBS over a 66 h period in a humidified incubator set at 37 °C with 5% CO<sub>2</sub>.

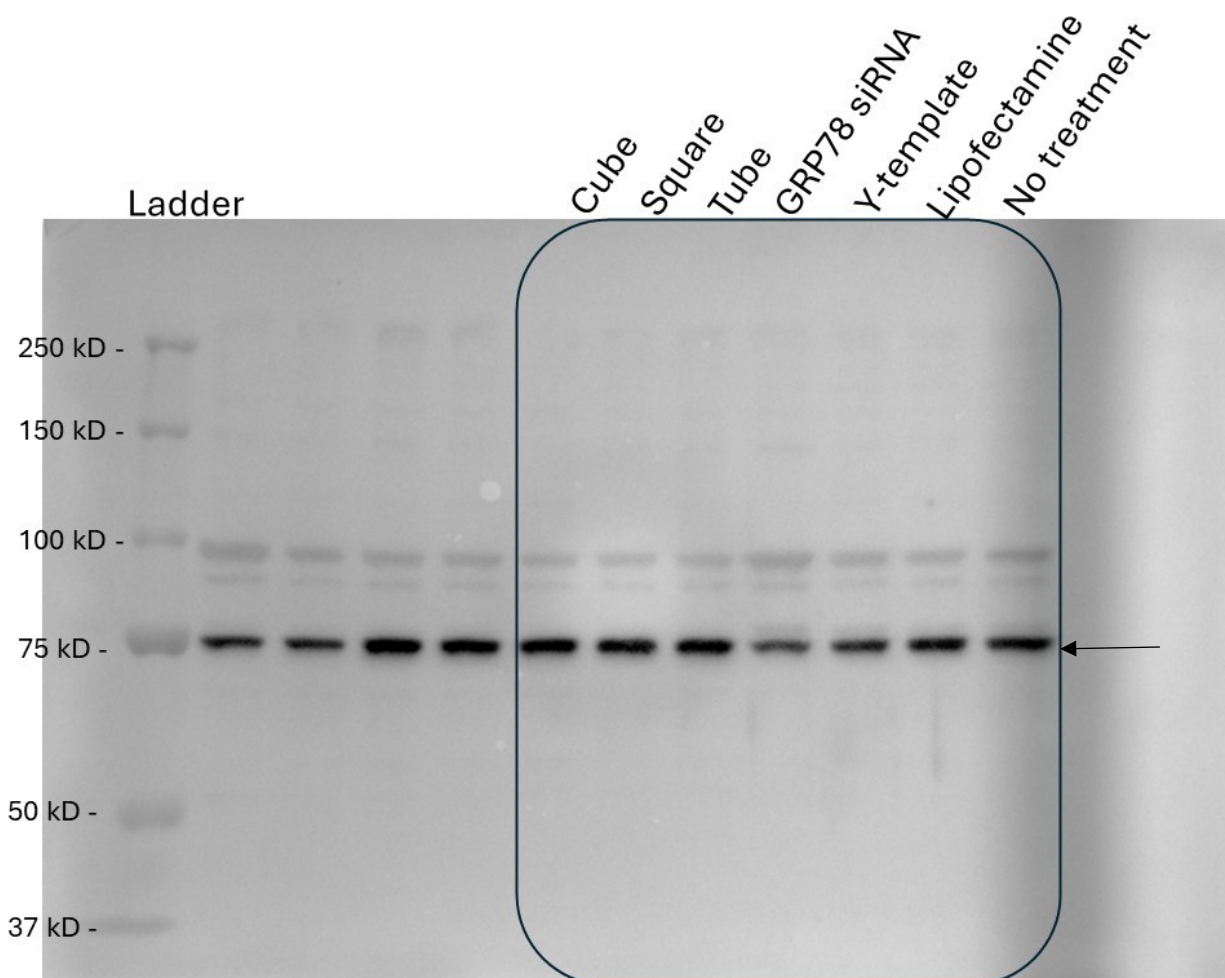


**Figure S32.** Full western blot image of GRP78 using primary monoclonal anti-GRP78 and HRP-conjugated secondary antibody following siRNA transfections (25 nM) of the siRNA nanostructures (cube, square and tube) along with GRP78 siRNA, Y-template and vehicle controls with Lipofectamine 3000™ (6  $\mu$ L) in DMEM cell culture media supplemented with 10% FBS over a 66 h period in a humidified incubator set at 37 °C with 5% CO<sub>2</sub>.

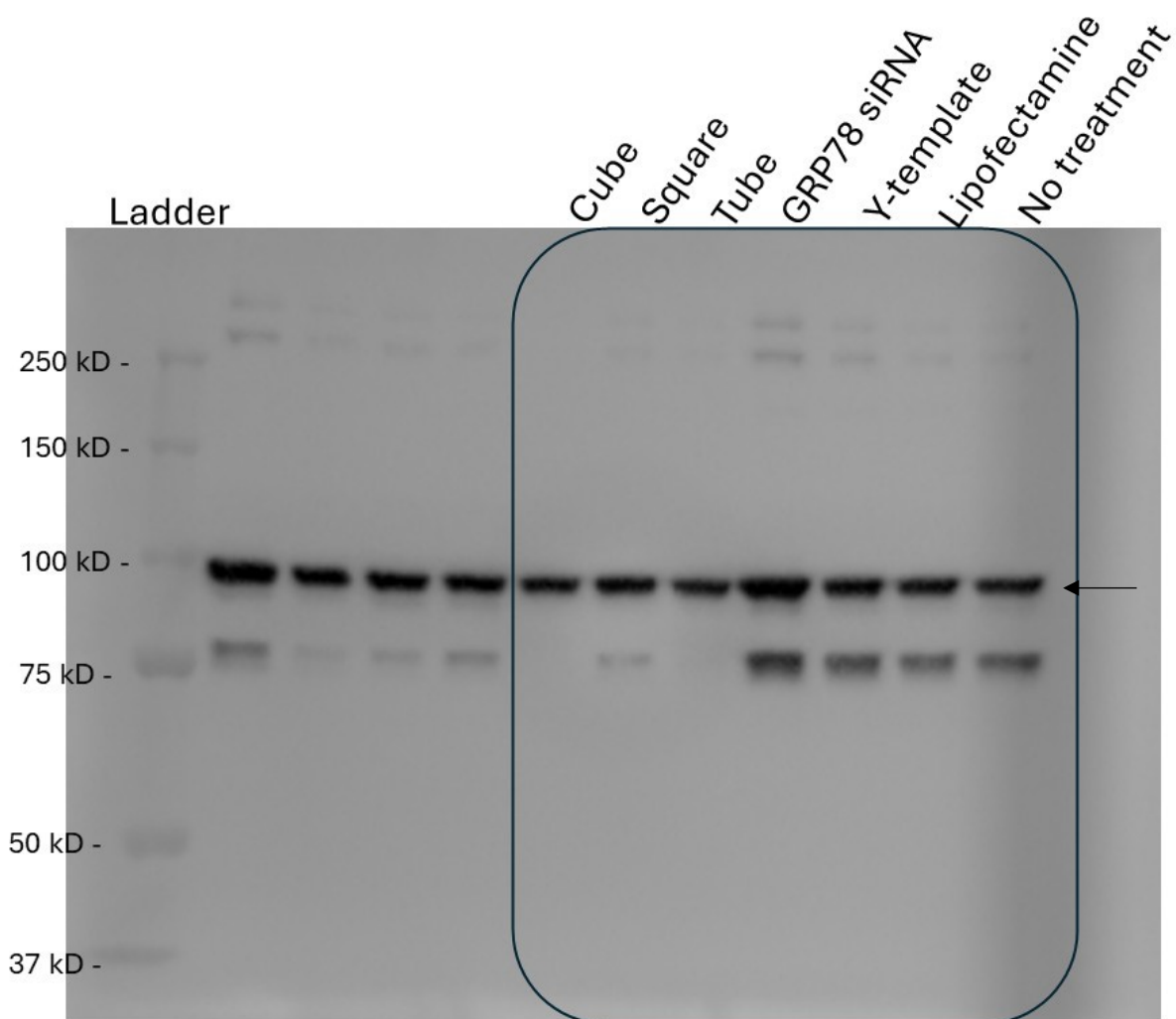


**Figure S33.** Full western blot image of GRP94 using primary monoclonal anti-GRP94 and HRP-conjugated secondary antibody following siRNA transfections (25 nM) of the siRNA nanostructures (cube, square and tube) along with GRP78 siRNA, Y-template and vehicle controls with Lipofectamine 3000™ (6  $\mu$ L) in DMEM cell culture media supplemented with 10% FBS over a 66 h period in a humidified incubator set at 37 °C with 5% CO<sub>2</sub>.

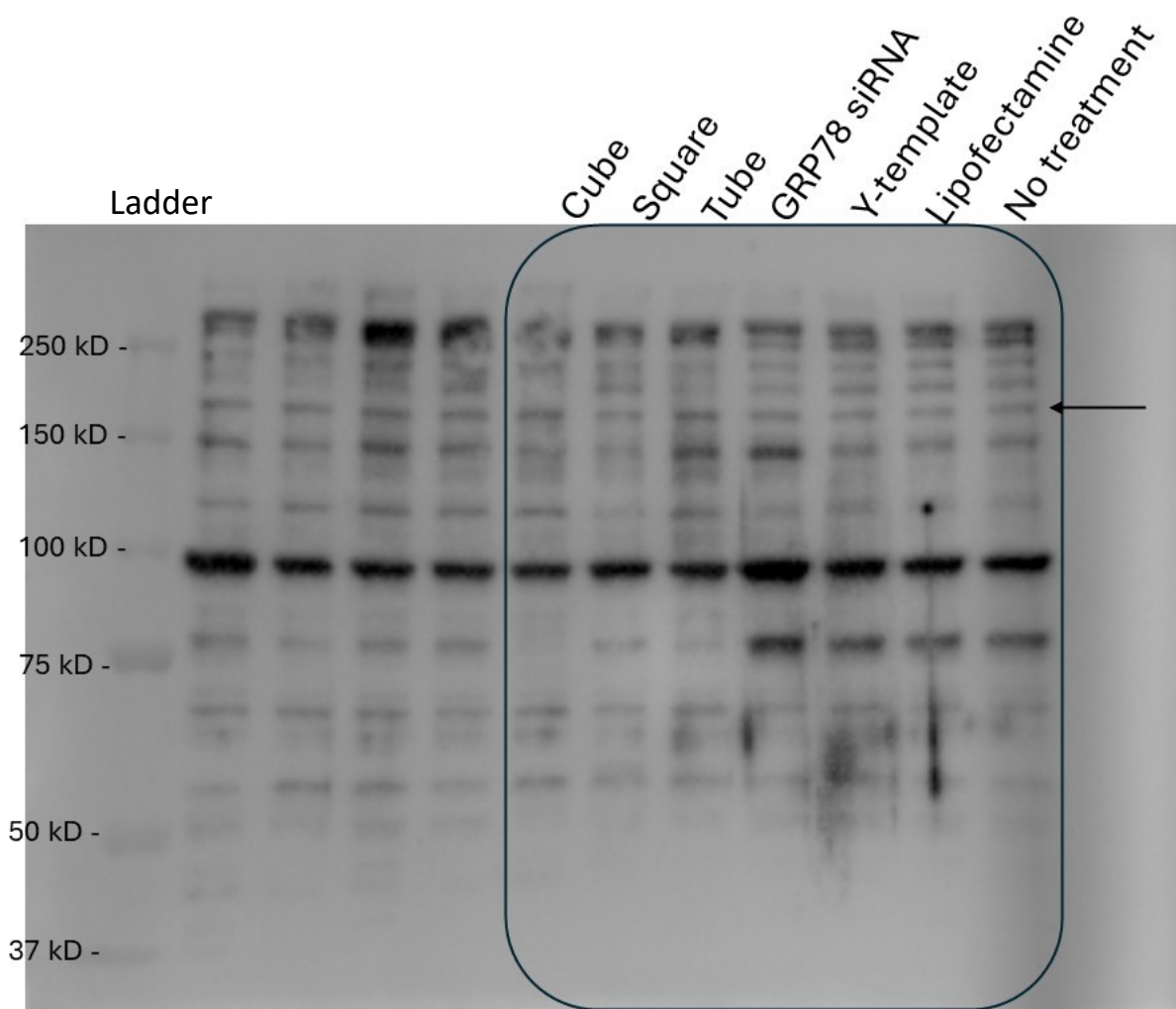


**Figure S34.** Full western blot image of GRP170 using primary monoclonal anti-GRP170 and HRP-conjugated secondary antibody following siRNA transfections (25 nM) of the siRNA nanostructures (cube, square and tube) along with GRP78 siRNA, Y-template and vehicle controls with Lipofectamine 3000™ (6 μL) in DMEM cell culture media supplemented with 10% FBS over a 66 h period in a humidified incubator set at 37 °C with 5% CO<sub>2</sub>.

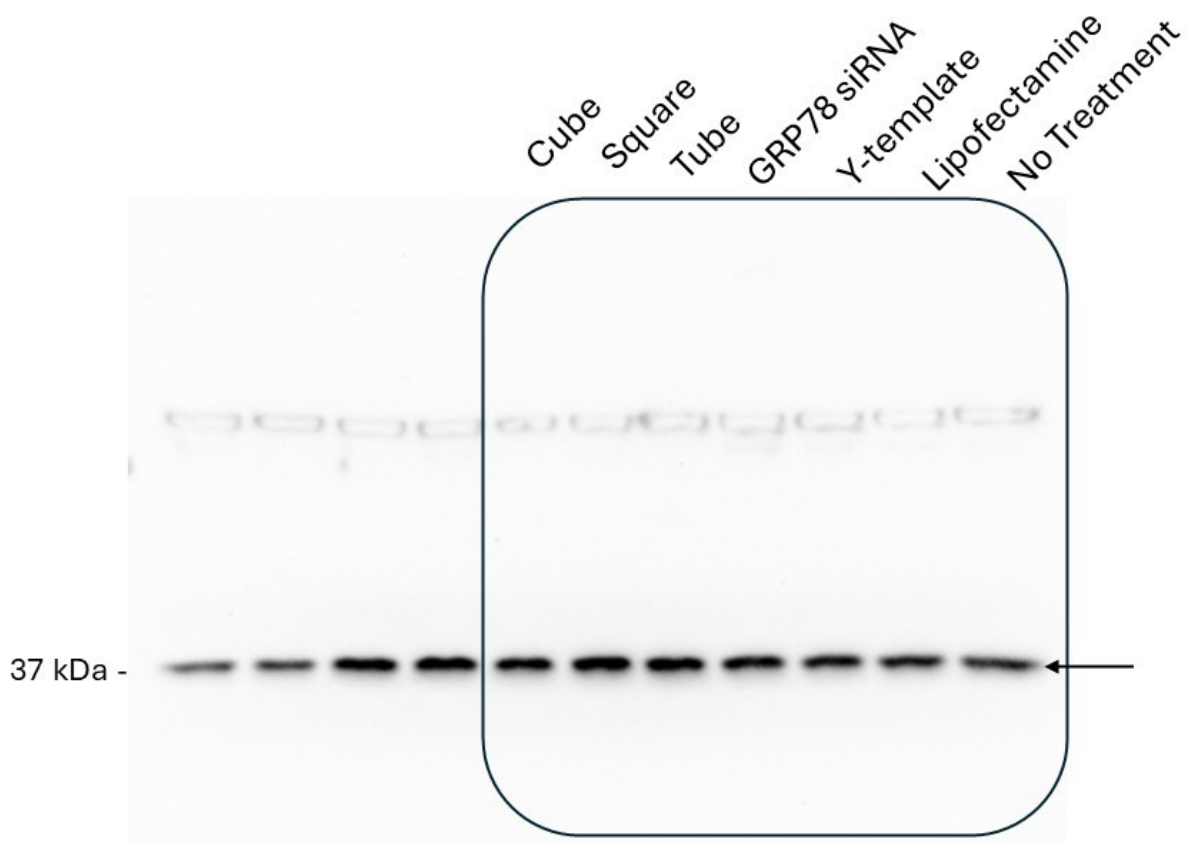


**Figure S35.** Full western blot image of housekeeping GAPDH as quantitative protein control using primary monoclonal anti-GAPDH and HRP-conjugated secondary antibody following siRNA transfections (25 nM) of the siRNA nanostructures (cube, square and tube) along with GRP78 siRNA, Y-template and vehicle controls with Lipofectamine 3000™ (6  $\mu$ L) in DMEM cell culture media supplemented with 10% FBS over a 66 h period in a humidified incubator set at 37 °C with 5% CO<sub>2</sub>.

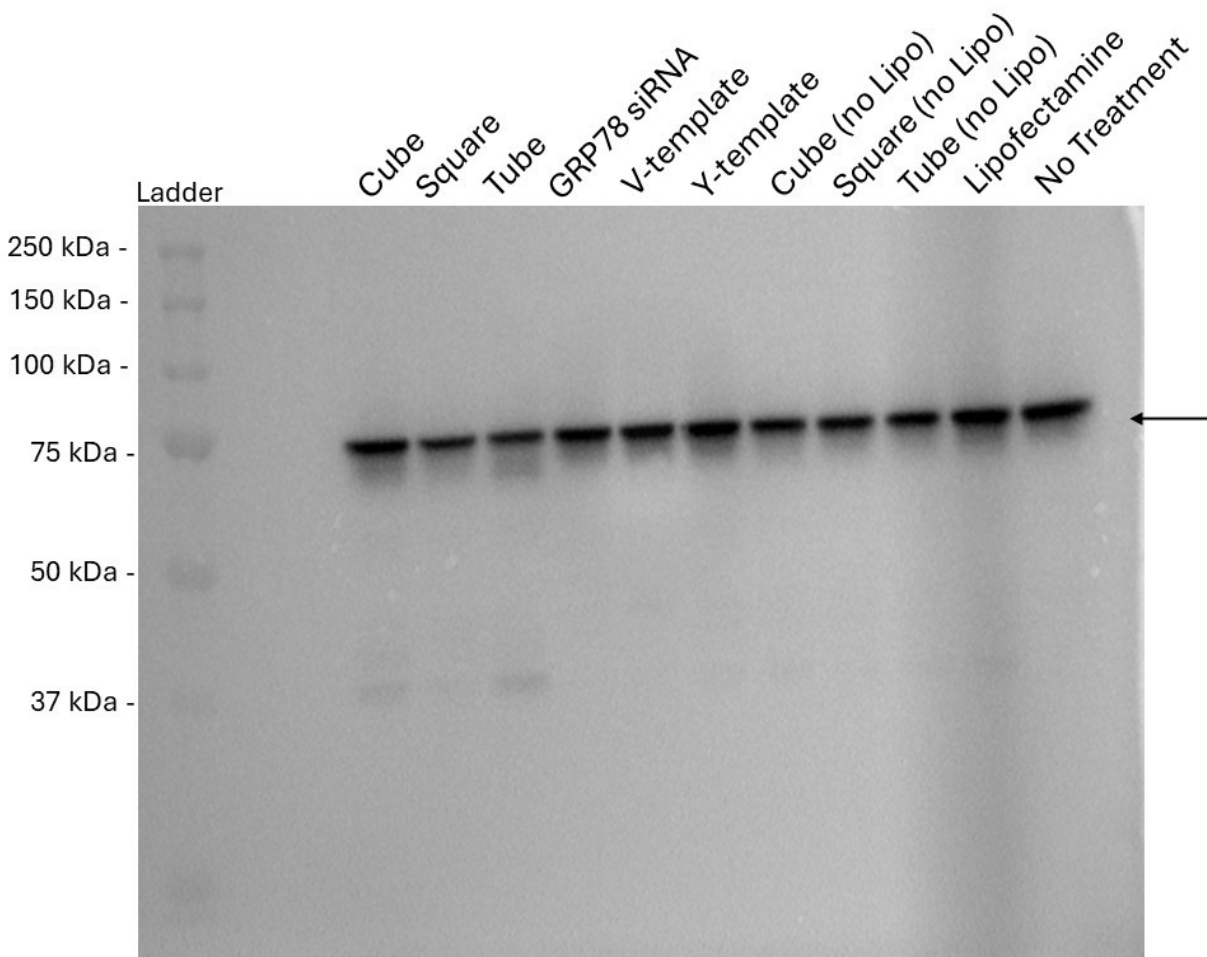


**Figure S36.** Full western blot image of GRP75 using primary monoclonal anti-GRP75 and HRP-conjugated secondary antibody following siRNA transfections (50 nM) of the siRNA nanostructures (cube, square and tube with and without Lipofectamine, Lipo) along with GRP78 siRNA, V-, Y-templates and vehicle controls with Lipofectamine 3000™ (4  $\mu$ L) in DMEM cell culture media supplemented with 10% FBS over a 66 h period in a humidified incubator set at 37 °C with 5% CO<sub>2</sub>.

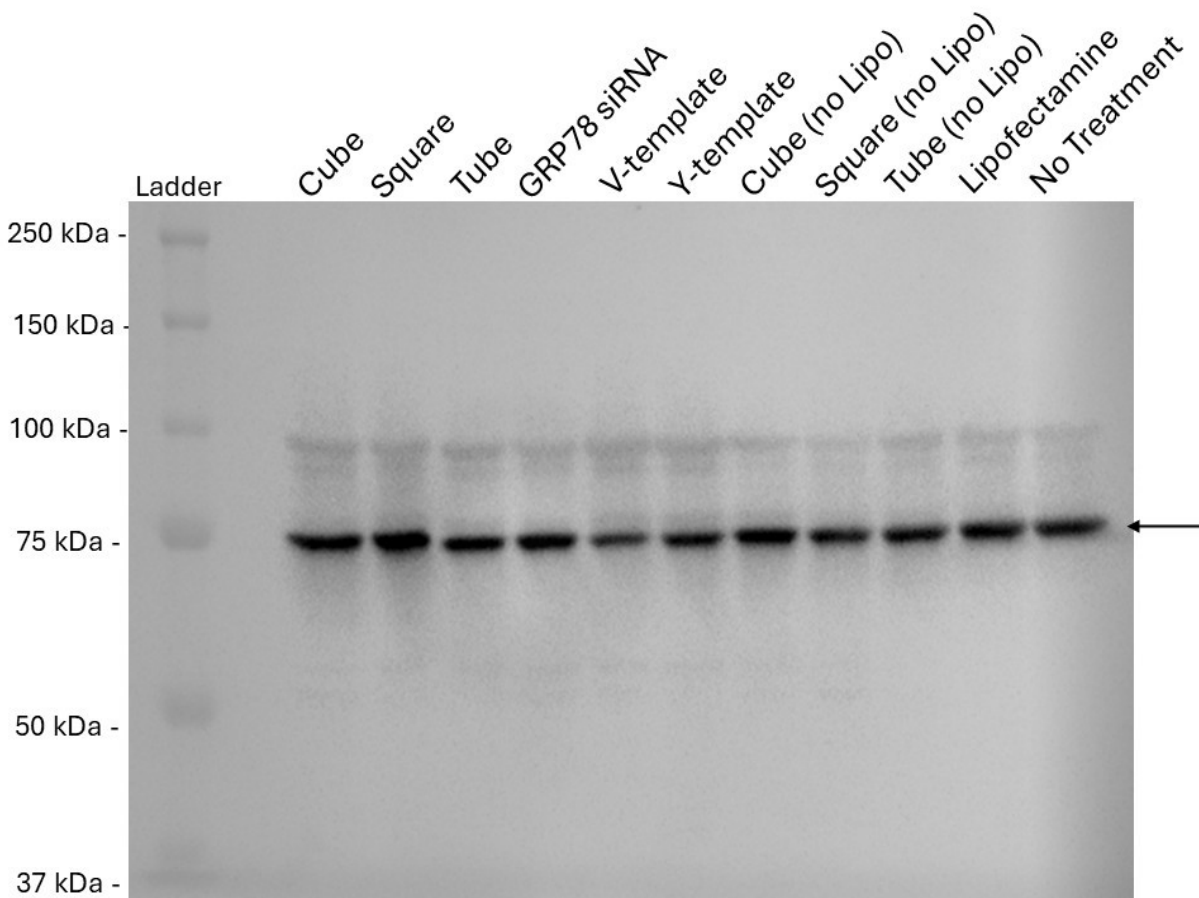


**Figure S37.** Full western blot image of GRP78 using primary monoclonal anti-GRP78 and HRP-conjugated secondary antibody following siRNA transfections (50 nM) of the siRNA nanostructures (cube, square and tube with and without Lipofectamine, Lipo) along with GRP78 siRNA, V-, Y-templates and vehicle controls with Lipofectamine 3000™ (4  $\mu$ L) in DMEM cell culture media supplemented with 10% FBS over a 66 h period in a humidified incubator set at 37 °C with 5% CO<sub>2</sub>.

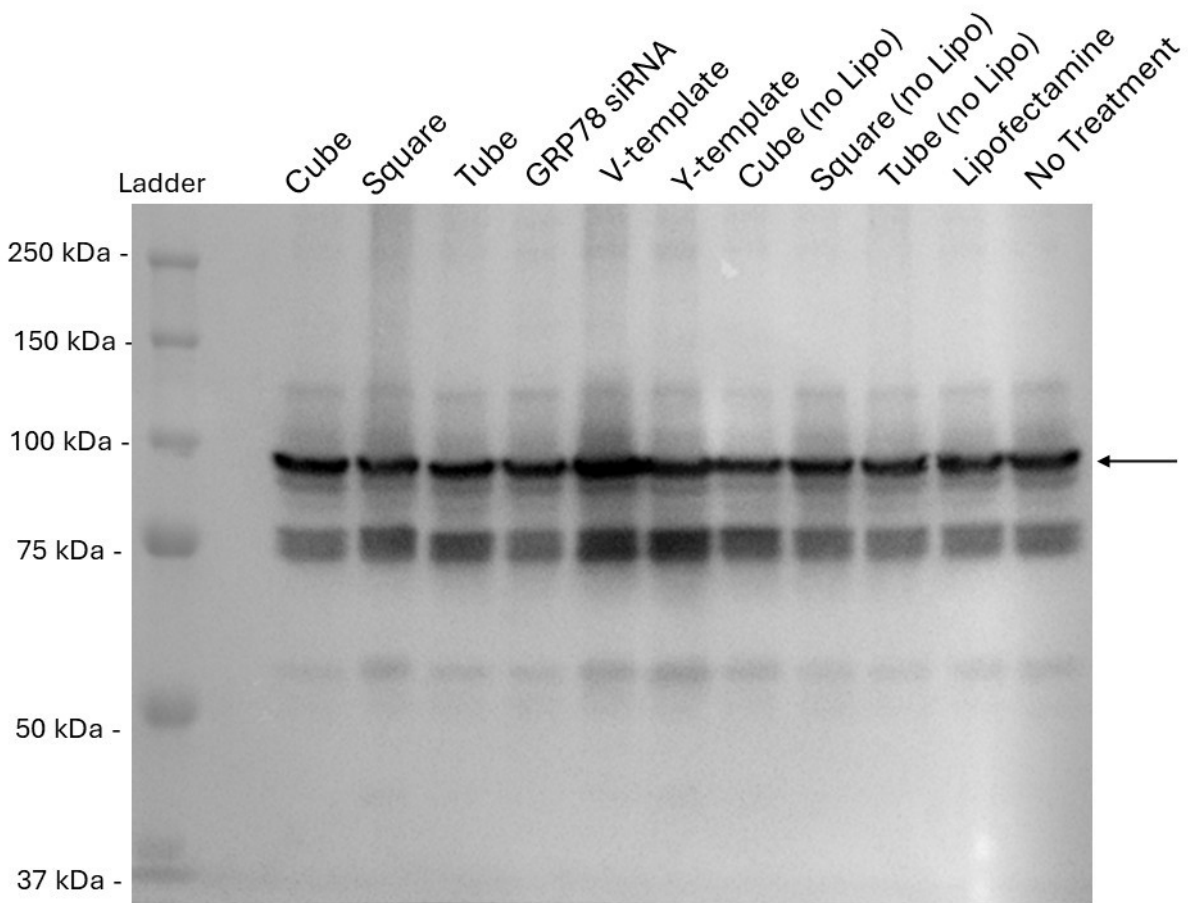


**Figure S38.** Full western blot image of GRP94 using primary monoclonal anti-GRP94 and HRP-conjugated secondary antibody following siRNA transfections (50 nM) of the siRNA nanostructures (cube, square and tube with and without Lipofectamine, Lipo) along with GRP78 siRNA, V-, Y-templates and vehicle controls with Lipofectamine 3000™ (4  $\mu$ L) in DMEM cell culture media supplemented with 10% FBS over a 66 h period in a humidified incubator set at 37 °C with 5% CO<sub>2</sub>.

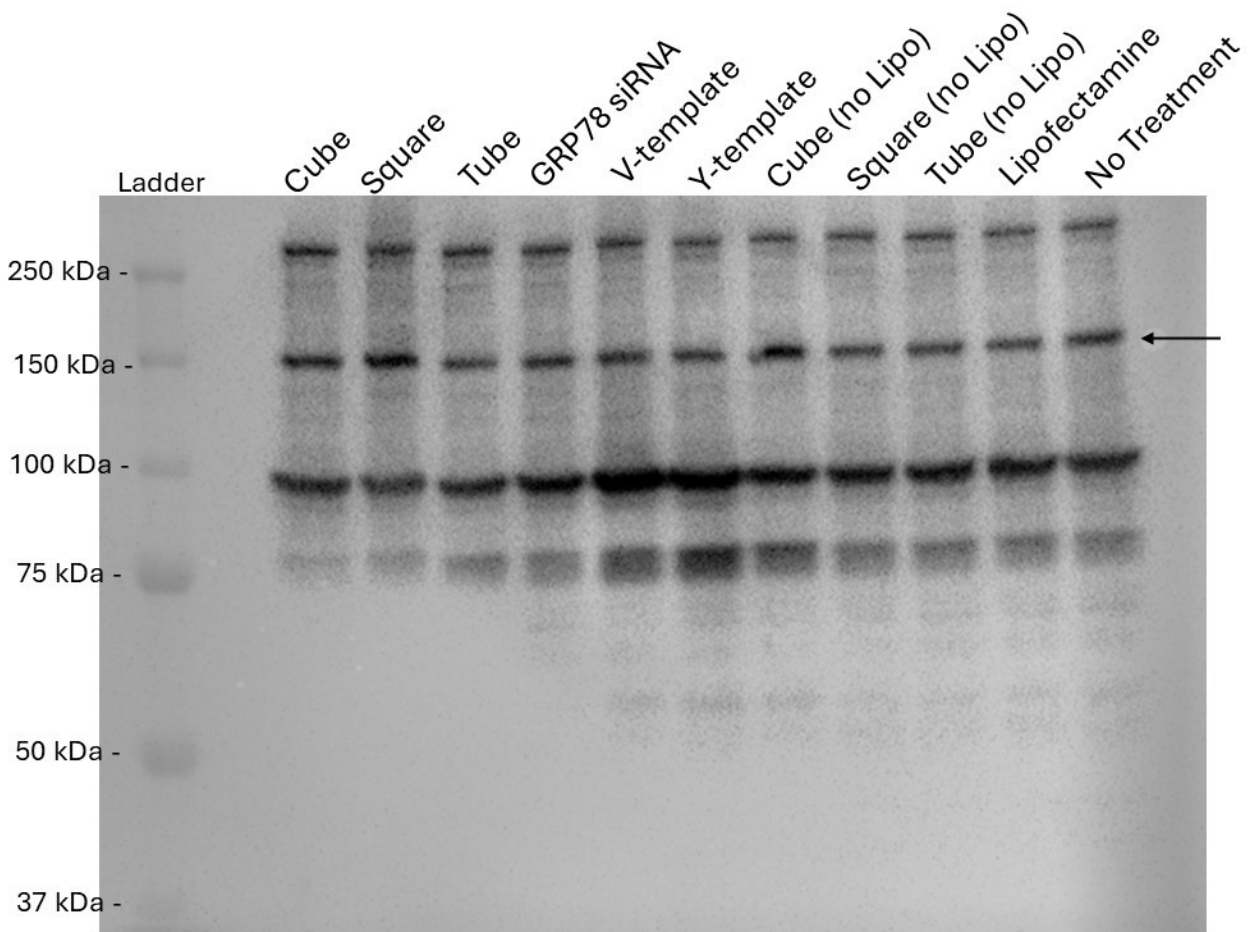


**Figure S39.** Full western blot image of GRP170 using primary monoclonal anti-GRP170 and HRP-conjugated secondary antibody following siRNA transfections (50 nM) of the siRNA nanostructures (cube, square and tube with and without Lipofectamine, Lipo) along with GRP78 siRNA, V-, Y-templates and vehicle controls with Lipofectamine 3000™ (4  $\mu$ L) in DMEM cell culture media supplemented with 10% FBS over a 66 h period in a humidified incubator set at 37 °C with 5% CO<sub>2</sub>.

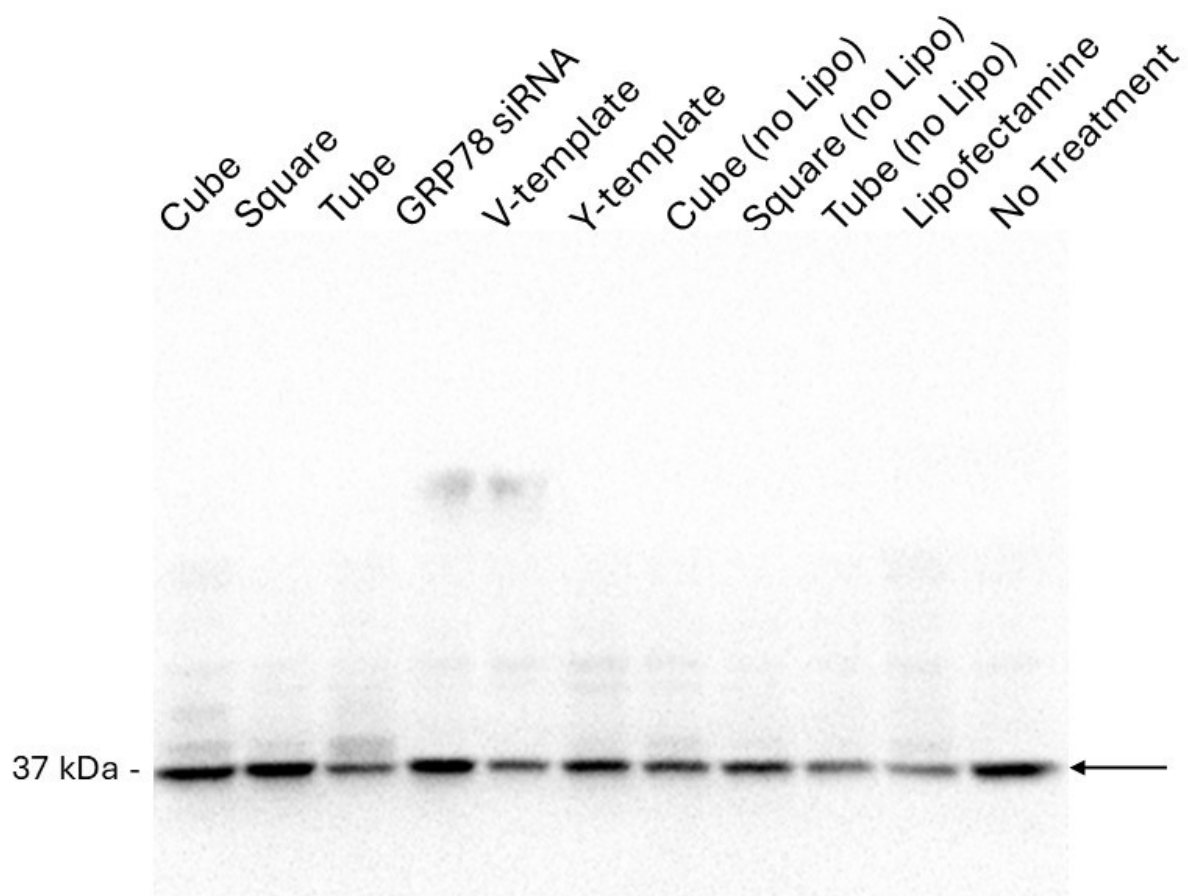
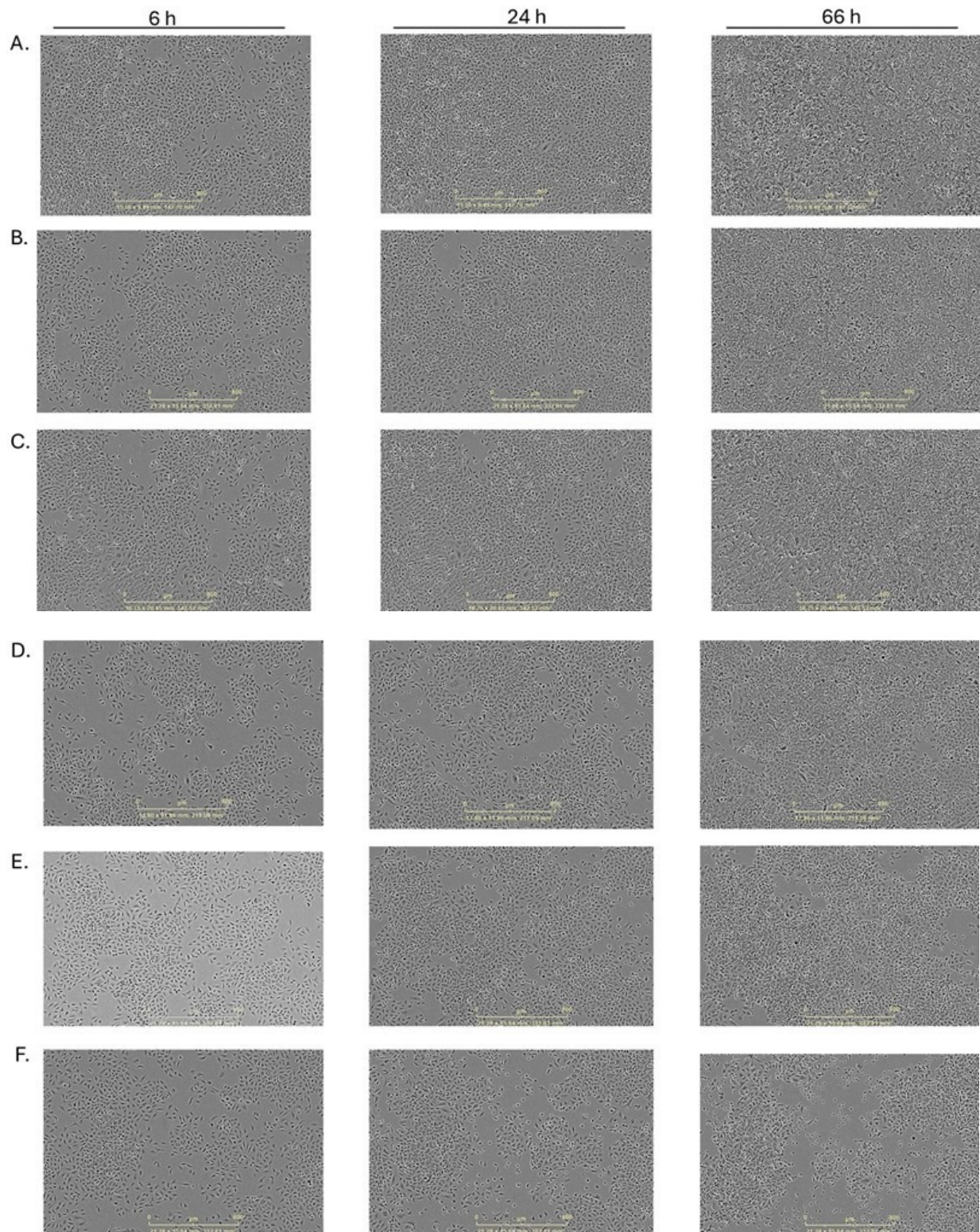


**Figure S40.** Full western blot image of housekeeping GAPDH as quantitative protein control using primary monoclonal anti-GAPDH and HRP-conjugated secondary antibody following siRNA transfections (50 nM) of the siRNA nanostructures (cube, square and tube with and without Lipofectamine, Lipo) along with GRP78 siRNA, V-, Y-templates and vehicle controls with Lipofectamine 3000™ (4  $\mu$ L) in DMEM cell culture media supplemented with 10% FBS over a 66 h period in a humidified incubator set at 37 °C with 5% CO<sub>2</sub>.



G.

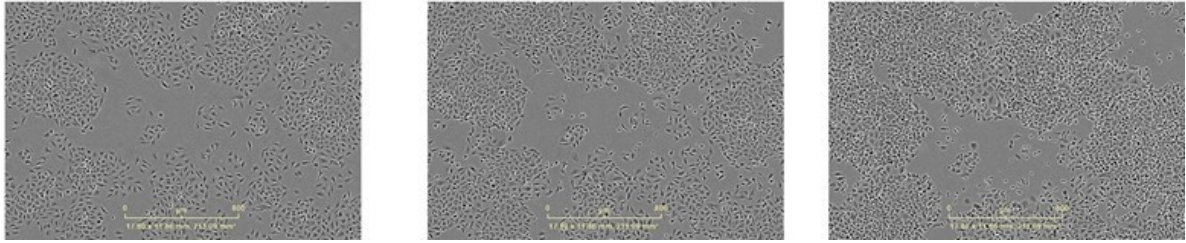


**Figure. S41.** Time point brightfield images demonstrating the changes in the A549 cell culture confluency during the siRNA (25 nM) transfection with Lipofectamine 3000™ (6  $\mu$ L) in DMEM cell culture media supplemented with 10% FBS during an incubation period of 66 h in a humidified incubator set at 37 °C with 5% CO<sub>2</sub>. Conditions (A) no treatment, A549 cells only, (B) vehicle, Lipofectamine 3000™ only, (C) Y-template RNA, (D) GRP78 siRNA, (E) GRP-siRNA nanosquare, (F) GRP-siRNA nanocube and (G) GRP-siRNA nanotube.